

**M.Sc. Physics**

**Anmol Aggarwal & Ashi Mittal**

**2023**

**QUANTUM EFFICIENCY OF ASTRONOMICAL CHARGE-  
COUPLED DEVICES FOR DEEPER EXPLORATION OF OUR  
COSMOS**

A DISSERTATION

SUBMITTED IN PARTIAL FULFILLMENT OF THE  
REQUIREMENTS FOR THE AWARD OF THE DEGREE OF

**MASTER OF SCIENCE**

**IN**

**PHYSICS**

Submitted By:

**ANMOL AGGARWAL & ASHI MITTAL**

**2K21/MSCPHY/55 & 2K21/MSCPHY/07**

Under the supervision of

Prof. (Dr.) NITIN K. PURI

Dr. GEORGE M. SEABROKE



**DEPARTMENT OF APPLIED  
PHYSICS**

**DELHI TECHNOLOGICAL  
UNIVERSITY**  
(Formerly Delhi College of Engineering)  
Bawana Road, Delhi-110042



**DEPARTMENT OF SPACE &  
CLIMATE PHYSICS**

**UNIVERSITY COLLEGE LONDON**  
Holmbury St. Mary, Dorking, Surrey  
United Kingdom- RH5 6NT

May, 2023

**QUANTUM EFFICIENCY OF  
ASTRONOMICAL CHARGE-COUPLED  
DEVICES FOR DEEPER EXPLORATION  
OF OUR COSMOS**

**DELHI TECHNOLOGICAL UNIVERSITY**

(Formerly Delhi College of Engineering)

Bawana Road, Delhi-110042

**CANDIDATE'S DECLARATION**

We, **Anmol Aggarwal & Ashi Mittal**, Roll Nos. **2K21/MSCPHY/55 & 2K21/MSCPHY/07** respectively, students of M.Sc. Physics hereby declare that the project Dissertation titled "**Quantum Efficiency of Astronomical Charge-coupled Devices for Deeper Exploration of our Cosmos**", which is submitted by us to the Department of Applied Physics, Delhi Technological University, Delhi in the partial fulfilment of the requirement for the award of the degree of Master of Science, is original and not copied from any source without proper citation. This work has not previously formed the basis for the award of any Degree, Diploma Associateship, Fellowship or other similar title or recognition.

Place: CERN, Switzerland

Date: 30<sup>th</sup> May 2023


Place: Delhi, India

Date: 30<sup>th</sup> May 2023



**ANMOL AGGARWAL**

**(2K21/MSCPHY/55)**



**ASHI MITTAL**

**(2K21/MSCPHY/07)**

**DELHI TECHNOLOGICAL UNIVERSITY**

(Formerly Delhi College of Engineering)


Bawana Road, Delhi-110042

**CERTIFICATE**

I hereby certify that the Project Dissertation titled “**Quantum Efficiency of Astronomical Charge-coupled Devices for Deeper Exploration of our Cosmos**” which is submitted by **Anmol Aggarwal & Ashi Mittal, Roll Nos. 2K21/MSCPHY/55 & 2K21/MSCPHY/07, Department of Applied Physics, Delhi Technological University, Delhi** in partial fulfilment of the requirement for the award of the degree of Master of Science, is a record of the project work carried out by the students under our supervision. To the best of our knowledge, this work has not been submitted in part or full for any Degree or Diploma to this University or elsewhere.

Place: Delhi, India

Date: 30 May 2023


  
**Prof. (Dr.) Nitin K. Puri**

**SUPERVISOR**

Professor  
Department of Applied Physics  
Delhi Technological University

Place: Newbury, United Kingdom

Date: 30 May 2023

  
**Dr. George M. Seabroke**

**CO-SUPERVISOR**

Principal Research Fellow  
Mullard Space Science Laboratory  
Department of Space and Climate Physics  
University College London

---

---

## ABSTRACT

When one looks up at the sky and counts the number of stars and observes constellations, they are not only appreciating the beauty of the universe but doing an astronomer's job as well. Astronomy is the oldest science that humans have dealt with, and it is rather the simplest science that can be done with the naked eye. Our quest to understand the nature of our existence started with the simple observation of celestial objects. With time humans were able to solve a lot of such mysteries and as we move on to the next job, it becomes more complex. In today's astronomical scenario, this quest is driven by the advancement in the technology used for observing our universe.

Charge-coupled devices (CCDs) are the backbone of all space study missions today, such as Gaia, Hubble Space Telescope, James Webb Telescope, etc. They are the basic piece of machinery used by any space mission to capture the light in space and help us create images that can be studied on Earth. Their functionality is what makes them an imperative instrument whose efficiency needs to be as high as possible. Hence this project is focused on finding ways to enhance

---

---

---

the quantum efficiency of Gaia Astrometric Field (AF) CCDs by altering some of their structural parameters.

CCDs lose a lot of incident photons due to optical losses. To reduce the loss anti-reflection (AR) coatings are applied on the substrate. Currently, hafnium dioxide ( $\text{HfO}_2$ ) is being used as an AR coating for the Gaia AF CCDs. Through our studies, we contemplated alternative AR coatings that could increase the QE of the CCDs. Aluminium oxide ( $\text{Al}_2\text{O}_3$ ), zinc sulphide ( $\text{ZnS}$ ), zirconium dioxide ( $\text{ZrO}_2$ ), and tantalum pentoxide ( $\text{Ta}_2\text{O}_5$ ) are some promising materials that have been selected and tested by us for the Gaia AF CCDs.

Further, gallium nitride (GaN) has been analysed as an alternative to silicon for its use in broadband astronomical CCDs. The optical and electronic performance of GaN and silicon CCD pixel models have been compared for this purpose.

Simulations have been conducted using the SILVACO TCAD software to test these coatings on the Gaia pixel structure. The Monte Carlo method has been implemented by SILVACO for these simulations. ATLAS module of the SILVACO software is employed for the model.

Upon contemplation, two AR coatings ( $\text{Ta}_2\text{O}_5$  and  $\text{ZrO}_2$ ) turn out to produce better results than  $\text{HfO}_2$ . They give better QE towards the lower end of the Gaia AF CCDs' operational spectrum (from  $0.330 \mu\text{m}$  to  $0.575 \mu\text{m}$ ) and prove to be better AR coatings for broadband astronomical CCDs. GaN also proves to be substantially better than silicon for use in such devices. These studies will open new avenues for understanding the evolution of the Milky Way and our universe.

---

## ACKNOWLEDGEMENT

There are a lot of people who helped us out from time to time and aided in the completion of this work. We are extremely grateful to all of them but first and foremost we would to express our immense gratitude towards our dissertation supervisor and our mentor, Prof. (Dr.) Nitin K. Puri. He has been there for us every step of the way to guide us through any kind of problem. He kept our morals high and taught us how to walk on the path of research at Delhi Technological University. His innovative pedagogy must be specially highlighted which not only enabled us to complete this work but also prepared us for our future research and life challenges.

We are extremely thankful to our dissertation co-supervisor, Dr. George M. Seabroke. He has been an incredible support throughout our research work. His expertise and experience in the subject matter provided us with invaluable insights and helped enhance our research quality. It is his work on the Gaia AF CCDs that inspired us to work in this direction.

We also extend our in-depth gratitude towards our friend and role model Dr. Ritika Khatri. She supported us in keeping our spirits high even when the times were very distressful. We would also like to thank our laboratory members and friends, Nikita Jain, Hemant Kumar Arora and Sunil Kumar, for their constant support and understanding.

Finally, we would like to thank our parents and family members whose blessings and constant affirmation made it possible for us to be capable enough to work at Delhi Technological University.

*Ashi Mittal*

**ASHI MITTAL**

*Anmol Aggarwal*

**ANMOL AGGARWAL**

---

## CONTENTS

| Title   | Page No. |
|---|----------|
| <b>Candidate's Declaration</b>                              | iii      |
| <b>Certificate</b>  | iv       |
| <b>Abstract</b>   | v        |
| <b>Acknowledgement</b>                                      | vii      |
| <b>Table of Contents</b>                                    | viii     |
| <b>List of Tables</b>                                       | xi       |
| <b>List of Figures</b>                                      | xii      |
| <b>List of Symbols, Abbreviations, and<br/>Nomenclature</b> | xvi      |
| <b>1. Introduction</b>                                      | 1        |
| 1.1 Structure of Charged Coupled Devices (CCDs)             | 1        |
| 1.2 Operation of CCDs                                       | 3        |
| 1.3 Types of CCDs   | 4        |
| 1.4 Importance of CCDs in Astronomy and<br>Astrophysics     | 5        |
| <b>2. Performance of CCDs</b>                               | 8        |
| 2.1 Quantum Efficiency (QE)                                 | 8        |
| 2.1.1 Internal Quantum Efficiency                           | 8        |
| 2.1.2 External Quantum Efficiency                           | 9        |
| 2.2 Factors Affecting Quantum Efficiency                    | 9        |
| 2.2.1 Real Refractive Index                                 | 9        |
| 2.2.2 Complex Refractive Index                              | 10       |
| 2.2.3 Thickness of the Substrate Material                   | 11       |
| 2.3 Conclusion  | 11       |
| <b>3. Anti-Reflection (AR) Coatings</b>                     | 12       |
| 3.1 Selecting the materials for AR coatings                 | 12       |
| 3.1.1 Reflectivity  | 13       |
| 3.1.2 Refractive Index Matching                             | 14       |
| 3.1.3 Absorption Coefficient                                | 18       |



---

|     |   |    |
|-----|---|----|
| 3.2 | Conclusion  | 19 |
| 4.  | <b>Benchmarking of the Gaia Astrometric Field</b>                                     | 20 |
|     | <b>CCD pixel structure using SILVACO</b>  |    |
| 4.1 | Gaia Pixel Structure  | 20 |
| 4.2 | Modelling Using SILVACO TCAD  | 22 |
| 4.3 | Comparison with reported External Quantum Efficiency                                  | 26 |
| 4.4 | Conclusion  | 27 |
| 5.  | <b>Study of the QE of the Gaia AF CCD pixel model with several AR coatings</b>        | 28 |
| 5.1 | With Hafnium Dioxide  | 28 |
| 5.2 | With Zinc Sulphide  | 29 |
| 5.3 | With Aluminium Oxide  | 30 |
| 5.4 | With Zirconium Dioxide  | 31 |
| 5.5 | With Tantalum Pentoxide   | 33 |
| 5.6 | Conclusion  | 35 |
| 6.  | <b>Analysis of gallium nitride as an alternative to silicon for astronomical CCDs</b> | 38 |
| 6.1 | Importance of imaginary refractive index  | 38 |
| 6.2 | Suitability of GaN for broadband astronomical CCDs                                    | 40 |
| 6.3 | Simulation and calculations for the GaN CCD pixel structure                           | 40 |
| 6.4 | Comparison of the GaN CCD model with the Gaia AF CCD model                            | 41 |
| 6.5 | Conclusion  | 44 |
| 7.  | <b>Conclusion and future scope of this work</b>                                       | 45 |
|     | <b>References</b>   | 47 |
|     | <b>Declaration and Certificate</b>  | 51 |
|     | <b>List of Publications</b>   | 53 |
|     | <b>Acceptance Proofs</b>  | 54 |

---

---

|                                      |    |
|--------------------------------------|----|
| <b>Journal Index Proof</b>           | 55 |
| <b>Plagiarism Report</b>             | 57 |
| <b>Accepted Research Article</b>     | 58 |
| <b>Communicated Research Article</b> | 67 |

---

## LIST OF TABLES

| <b>S.No.</b> | <b>Table No.</b> | <b>Title of the Table</b>  | <b>Page No.</b> |
|--------------|------------------|--|-----------------|
| <b>1.</b>    | <b>Table 4.1</b> | The thickness and doping densities of different layers in the AF CCD pixel structure.  | 23              |
| <b>2.</b>    | <b>Table 4.2</b> | List of theoretical and experimental constants.  | 24              |
| <b>4.</b>    | <b>Table 5.1</b> | Percentage increment and decrement in the QE of the Gaia AF CCD with different AR coatings as compared to the HfO <sub>2</sub> AR coating. | 35              |

---

## LIST OF FIGURES

| <b>S. No.</b> | <b>Fig. No.</b> | <b>Title of the Figure</b>  | <b>Page No.</b> |
|---------------|-----------------|---|-----------------|
| 1.            | Fig. 1.1        | Schematic of a basic MOS structure  | 2               |
| 2.            | Fig. 1.2        | Schematic of (a) SCCD; (b) BCCD   | 2               |
| 3.            | Fig. 1.3        | Charge transfer mechanism in a CCD  | 3               |
| 4.            | Fig. 1.4        | Front-illuminated CCD (Left); Back-illuminated CCD (Right)  | 5               |
| 5.            | Fig. 3.1        | Reflectivity of the CCD surface without any AR coating and with different AR coatings   | 13              |
| 6.            | Fig. 3.2        | Comparison of the refractive index of HfO <sub>2</sub> with the square root of the refractive index of silicon at different wavelengths               | 14              |
| 7.            | Fig. 3.3        | Comparison of the refractive index of ZnS with the square root of the refractive index of silicon at different wavelengths                            | 15              |
| 8.            | Fig. 3.4        | Comparison of the refractive index of Al <sub>2</sub> O <sub>3</sub> with the square root of the refractive index of silicon at different wavelengths | 16              |
| 9.            | Fig. 3.5        | Comparison of the refractive index of ZrO <sub>2</sub> with the square root of the refractive index of silicon at different wavelengths               | 17              |
| 10.           | Fig. 3.6        | Comparison of the refractive index of Ta <sub>2</sub> O <sub>5</sub>  | 18              |

---

|            |                 |  |    |
|------------|-----------------|--|----|
|            |                 | with the square root of the refractive index of silicon at different wavelengths   |    |
| <b>11.</b> | <b>Fig. 3.7</b> | The absorption coefficient of silicon <b>(a)</b> with AR coatings, <b>(b)</b> without AR coatings and <b>(c)</b> with and without AR coatings  | 19 |
| <b>12.</b> | <b>Fig. 4.1</b> | The Gaia Focal Plane has 106 CCDs arranged in seven different rows. The red rectangles represent radial velocity spectrometers (RVS). The green and yellow rectangles depict blue and red photometers (BP and RP) respectively, while the grey and black rectangles show wavefront sensors (WFS) and basic angle monitors (BAM) respectively. The light blue rectangles depict the most abundant i.e., AF CCDs and the dark blue rectangles are called sky mappers (SM). The SM and the WFS are also AF CCDs. The RVS and BAM have a construction similar to the RP. | 22 |
| <b>13.</b> | <b>Fig. 4.2</b> | Structure of a single pixel of the Gaia AF CCD (all the measurements are in $\mu\text{m}$ )  | 23 |
| <b>14.</b> | <b>Fig. 4.3</b> | The 2D Gaia AF CCD structure in the Across Scan (AC) direction as simulated in SILVACO ATLAS.  | 25 |
| <b>15.</b> | <b>Fig. 4.4</b> | Comparison of the actual EQE of the Gaia AF CCDs and the EQE obtained from the   | 27 |

|            |                 |   |    |
|------------|-----------------|---|----|
|            |                 | simulations   |    |
| <b>16.</b> | <b>Fig. 5.1</b> | QE of the Gaia AF CCD without and with an HfO <sub>2</sub> AR coating   | 29 |
| <b>17.</b> | <b>Fig. 5.2</b> | QE of the Gaia AF CCD without an AR coating, with an HfO <sub>2</sub> AR coating, and with a ZnS AR coating   | 30 |
| <b>18.</b> | <b>Fig. 5.3</b> | QE of the Gaia AF CCD without an AR coating, with an HfO <sub>2</sub> AR coating, and with an Al <sub>2</sub> O <sub>3</sub> AR coating                                 | 31 |
| <b>19.</b> | <b>Fig. 5.4</b> | QE of the Gaia AF CCD without an AR coating, with an HfO <sub>2</sub> AR coating, and with an ZrO <sub>2</sub> AR coating centred at 0.65 μm                            | 32 |
| <b>20.</b> | <b>Fig. 5.5</b> | QE of the Gaia AF CCD without an AR coating, with an HfO <sub>2</sub> AR coating, and with an ZrO <sub>2</sub> AR coating centred at 0.625 μm                           | 33 |
| <b>21.</b> | <b>Fig. 5.6</b> | QE of the Gaia AF CCD without an AR coating, with an HfO <sub>2</sub> AR coating, and with an Ta <sub>2</sub> O <sub>5</sub> AR coating centred at 0.65 μm              | 34 |
| <b>22.</b> | <b>Fig. 5.7</b> | QE of the Gaia AF CCD without an AR coating, with an HfO <sub>2</sub> AR coating, and with a Ta <sub>2</sub> O <sub>5</sub> AR coating centred at 0.625 μm              | 35 |
| <b>23.</b> | <b>Fig. 6.1</b> | The real (n) and imaginary refractive indices (k) of (a) silicon, (b) silicon carbide (SiC), and (c) gallium nitride (GaN) in the wavelength range of 0.2 μm to 0.8 μm. | 39 |

---

|     |                 |  |    |
|-----|-----------------|--|----|
| 24. | <b>Fig. 6.2</b> | The potential variation of the silicon Gaia AF CCD pixel model   | 42 |
| 25. | <b>Fig. 6.3</b> | The potential variation of the GaN pixel model   | 42 |
| 26. | <b>Fig. 6.4</b> | Comparison of the IQE and EQE of the GaN model with the silicon pixel model when they are simulated <b>(a)</b> Without any AR coatings, <b>(b)</b> with only silicon model with an HfO <sub>2</sub> coating, and <b>(c)</b> with GaN model with an Al <sub>2</sub> O <sub>3</sub> AR coating and silicon model with an HfO <sub>2</sub> AR coating | 43 |

---

**LIST OF SYMBOLS, ABBREVIATIONS, AND  
NOMENCLATURE**

| <b>S. No.</b> | <b>Acronym/Symbols</b>         | <b>Full Form</b>              |
|---------------|--------------------------------|-------------------------------|
| 1.            | CCD                            | Charge-Coupled Device         |
| 2.            | MOS                            | Metal-Oxide-Semiconductor     |
| 3.            | SCCD                           | Surface Channel CCD           |
| 4.            | BCCD                           | Buried Channel CCD            |
| 5.            | CTI                            | Charge Transfer Inefficiency  |
| 6.            | SiO <sub>2</sub>               | Silicon Dioxide               |
| 7.            | QE                             | Quantum Efficiency            |
| 8.            | AR                             | Anti-Reflection               |
| 9.            | IQE                            | Internal Quantum Efficiency   |
| 10.           | EQE                            | External Quantum Efficiency   |
| 11.           | R <sub>0</sub>                 | Reflectivity                  |
| 12.           | $\alpha$                       | Absorption Coefficient        |
| 13.           | JWST                           | James Webb Space Telescope    |
| 14.           | HfO <sub>2</sub>               | Hafnium Dioxide               |
| 15.           | AF                             | Astrometric Field             |
| 16.           | Al <sub>2</sub> O <sub>3</sub> | Aluminium Oxide               |
| 17.           | ZnS                            | Zinc Sulphide                 |
| 18.           | ZrO <sub>2</sub>               | Zirconium Dioxide             |
| 19.           | Ta <sub>2</sub> O <sub>5</sub> | Tantalum Pentoxide            |
| 20.           | ESA                            | European Space Agency         |
| 21.           | RP                             | Red Photometer                |
| 22.           | BP                             | Blue Photometer               |
| 23.           | RVS                            | Radial Velocity Spectrometers |
| 24.           | WFS                            | Wavefront Sensors             |
| 25.           | BAM                            | Basic Angle Monitors          |
| 26.           | SM                             | Sky Mapper                    |
| 27.           | J <sub>available</sub>         | Available Current Density     |



---

|     |                     |                                  |
|-----|---------------------|----------------------------------|
| 28. | $J_{\text{source}}$ | Source Current Density           |
| 29. | $J_n$               | Electron Current Density         |
| 30. | AC                  | Across Scan                      |
| 31. | ABD                 | Anti-Blooming Drain              |
| 32. | $E_g$               | Energy Gap of silicon            |
| 33. | $\epsilon_r$        | Relative Permittivity of silicon |
| 34. | X                   | Electron Affinity of silicon     |
| 35. | T                   | Temperature                      |
| 36. | GaN                 | Gallium Nitride                  |
| 37. | SiC                 | Silicon Carbide                  |
| 38. | K                   | Kelvins                          |
| 39. | V                   | Volts                            |
| 40. | eV                  | Electron volts                   |
| 41. | nm                  | Nanometres                       |
| 42. | $\mu\text{m}$       | Micrometres                      |
| 43. | AL                  | Along Scan                       |
| 44. | n                   | Real refractive index            |
| 45. | k                   | Imaginary refractive index       |
| 46. | $\lambda$           | Wavelength                       |
| 47. | $\pi$               | Pi                               |
| 48. | %                   | Percent                          |
| 49. | $\mu\text{s}$       | Microseconds                     |
| 50. | FPA                 | Focal Plane Array                |
| 51. | mm                  | Millimetres                      |
| 52. | 2D                  | 2 dimensions                     |
| 53. | $\text{cm}^3$       | Per centimetre cube              |
| 54. | >                   | Greater than                     |
| 55. | <                   | Less than                        |

---

---

# CHAPTER 1

## INTRODUCTION

A charge-coupled device (CCD) is used for digital image formation. It is based on the concept of photogeneration similar to that of the photoelectric effect [1-4]. While the photoelectric effect is generally exhibited by metals, the photogeneration in a CCD takes place inside a semiconductor.

In order to understand its working, one can use the concept of electrons and holes in semiconductors. When a photon is incident on the semiconductor surface it penetrates into the depletion region of the semiconductor substrate, if its energy is sufficiently high it then produces an electron-hole pair.

The construction, working, types, and relevance of CCD in the field of astronomy and astrophysics have been discussed in the subsequent sections in detail.

### 1.1 STRUCTURE OF A CHARGED COUPLED DEVICE

A CCD is a metal-oxide-semiconductor (MOS) based device, which utilises the field effect of electric potential [1, 4, 5]. It usually has a layer of

semiconductor and a conducting material separated by an insulating layer. The electrodes are not in direct contact with the semiconductor and the field effect properties of the electric potential are utilized [1, 4, 5]. The basic MOS structure can be seen in **Fig. 1.1**.

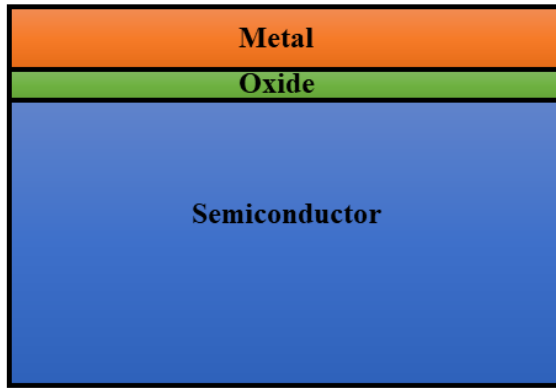


**Fig. 1.1:** Schematic of a basic MOS structure

The semiconductor layer of a CCD referred to as the substrate is either negatively doped, positively doped, or a p-n junction. A CCD that has only an n-type or p-type substrate is operated as a surface channel CCD (SCCD) [1, 6-8]. In an SCCD, the charge packet of the photogenerated charge carriers travels just underneath the insulating layer while being read out [1, 6-8]. If a p-n junction is used as a substrate in a CCD, then it is operated as a buried channel CCD (BCCD) [1, 7-9]. In a BCCD, the charge packet travels at a certain depth below the insulating layer while being read out [1, 7-9]. These CCDs have been represented in **Fig. 1.2**.

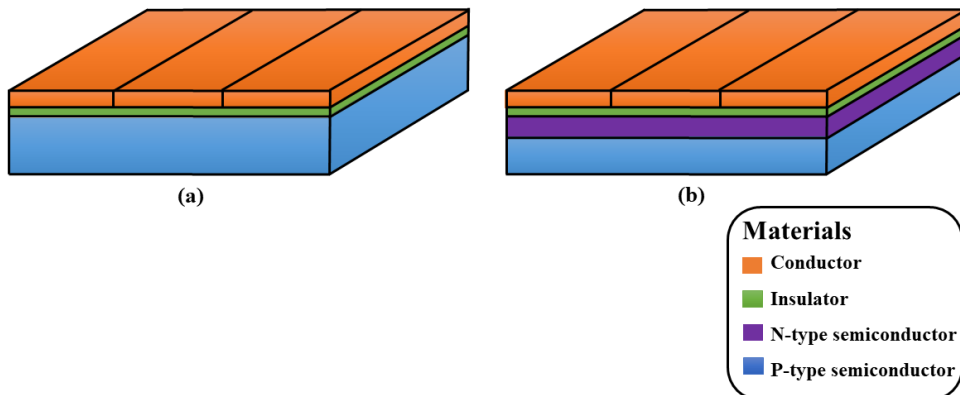


**Fig. 1.2:** Schematic of (a) SCCD; (b) BCCD

---

A BCCD is used for practical purposes because it offers two main advantages over an SCCD. An SCCD introduces charge transfer inefficiency (CTI) and dark current at the substrate-insulator interface [2, 3]. The substrate-insulator interface in an SCCD captures the charge carriers while they are being held by the potential on the electrode and releases them at a later time which causes CTI. It introduces dark current due to surface generation. These problems are nearly non-existent in a BCCD [2, 3, 10].

Realistically, a CCD has several electrodes, which allow it to read out the photogenerated electrons by varying the applied potential on the electrodes [2]. Generally, a CCD has a silicon substrate, silicon dioxide ( $\text{SiO}_2$ ) as an insulator and polysilicon electrodes. The reason for using  $\text{SiO}_2$  as an insulator is that while fabricating such CCDs, the silicon substrate has to be simply oxidised to obtain this insulating layer.

## 1.2 OPERATION OF CCDs

A CCD uses electrical potential to generate a neutral region free of electrons and holes. This region is called the depletion region. When a photon with energy greater than the material bandgap is incident on this region it produces an electron-hole pair [1-4].

In the case of an SCCD the generated photoelectrons travel to the substrate-insulator interface because of the electrode potential [2, 3]. They are then read out with the help of a series of electrodes by varying their alternating potential [1-4]. This process can be understood in **Fig. 1.3**.

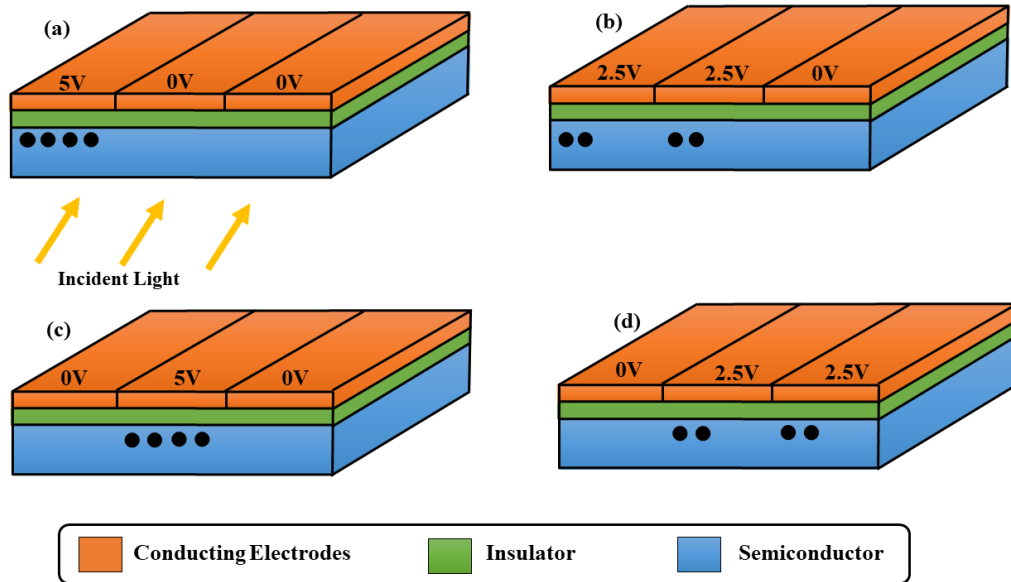


**Fig. 1.3:** Charge transfer mechanism in a CCD

In the case of a BCCD, the generated photoelectrons are held some distance below the substrate-insulator interface by reverse biasing the p-n junction. The same process, as is used for an SCCD, is followed by the BCCD to read out the charge packet produced.

### 1.3 TYPES OF CCDs

CCDs are broadly classified into two categories based on their illumination. Namely, front-illuminated and back-illuminated CCDs. The front-illuminated CCDs are those CCDs on which the light is incident from the electrode side, while the back-illuminated CCDs are illuminated from the substrate side [1-3].

While front-illuminated CCDs are easy to fabricate on a silicon wafer directly and are cheaper than back-illuminated CCDs, they offer many disadvantages. The electrodes of such CCDs absorb the blue and UV light almost completely hence they cannot be used to sense light of wavelengths shorter than 400 nm [2, 3]. They also offer very less quantum efficiency (QE) because of the

---

reflections from the substrate-insulator interface. The back-illuminated CCDs do not offer any such problems.

The QE in the case of back-illuminated CCDs is much greater which enhances the precision of the photodetector. The only losses that occur in this case are due to the reflection from the substrate surface, which can be reduced by applying appropriate Anti-Reflection (AR) Coatings [2, 3, 11]. At times, the substrate of back-illuminated CCDs is made to be quite thin, which causes interference fringing. This problem has been solved but increasing the thickness of the substrate layer and applying suitable AR coatings [2, 3, 11]. Hence back-illuminated CCDs are used for almost all applications in real life. Even though they are more expensive to fabricate, their performance justifies their cost. A schematic depicting the front and back-illuminated CCDs can be seen in **Fig. 1.4**.

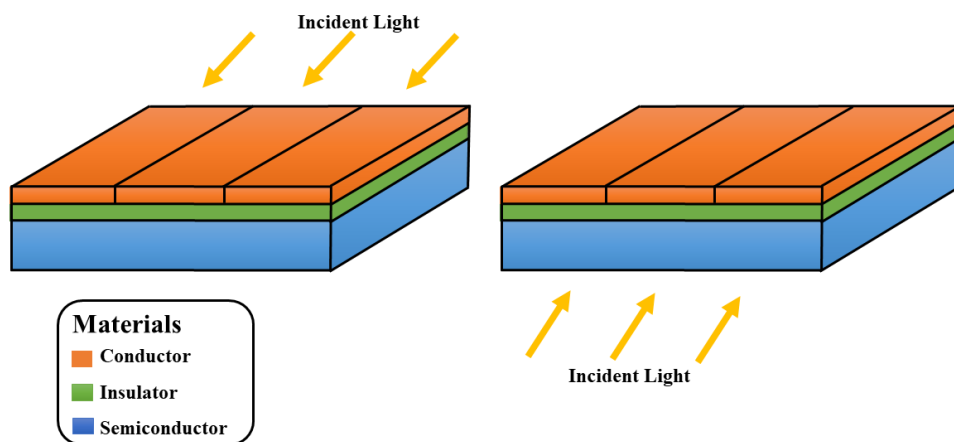


**Fig. 1.4:** Front-illuminated CCD (Left); Back-illuminated CCD (Right)

## 1.4 IMPORTANCE OF CCDS IN ASTRONOMY AND ASTROPHYSICS

Electromagnetic radiation which is light is one of the most important physical phenomena that has led to the exponential growth of our understanding of the universe and its physical and chemical properties. It is because the human eye is a natural detector of light, astronomy is the oldest science, which is built and driven by this physical entity.

---

During the early years of astronomy, only heavenly bodies that are visible to the naked eye could be observed by astronomers. Due to the unavailability of complex optical devices, they were only able to obtain limited information from these bodies. For example, information about seasons and time.

The invention of optical telescopes in the 17<sup>th</sup> century enabled astronomers to observe lights which are not very intense. They offered higher light collecting capacity, resolution, etc. The first challenge to the theory of geocentrism was also brought with the help of the very first optical telescopes designed by Galileo Galilei [12].

With the advent of electronic techniques and devices the horizon of astronomy expanded far outside the visible range of light. For the first time astronomers were able to observe radiation invisible to the human eye such as radio waves, infra-red waves, etc.

Despite such advances in the field of astronomy and astrophysics, astronomers still faced the dilemma of storing their optical observations digitally to analyse them and obtain constructive results.

The northern lights or aurora borealis is the effect, which might make anyone feel ecstatic but is a pure nuisance from an astronomical point of view. It is produced by the interaction of the earth's atmosphere and high energy radiation from the space; hence such radiations are not able to reach the surface of the earth and can only be observed from space. Due to many such reasons, the astronomers were prompted to design electronic photodetectors.

These days, the CCD photodetectors form the backbone of astronomy [3]. Not only they allow the storage of optical astronomical data digitally, they also enable astronomers to make observations from the space. This development also made the study of high energy radiation such as ultra-violet and gamma rays possible which were otherwise hazardous to the human eye and can only be observed from space.

CCDs are employed extensively by all the space missions to obtain several types of astronomical data such spectroscopic information of stars and the

---

---

interstellar medium, radial velocities, etc. Hence, CCDs can be classified as a cornerstone of modern-day astronomy.



---

## CHAPTER 2

### PERFORMANCE OF CCDs

The performance of CCDs is dependent on several factors. The primary factors that affect the performance are the refractive index and the thickness of the substrate material [3].

In this chapter, the QE of the CCDs, which is a standard parameter used to determine the performance of a CCD has been discussed. Usually, the higher the value of QE, the better the CCD.

#### 2.1 QUANTUM EFFICIENCY

The QE is a quantitative parameter dependent on incident photons which is used to judge the performance of optical devices such as solar cells and CCDs. It has two types, internal and external [13]. Both are slightly different but are used extensively to describe the performance of optical devices. The value of QE can reach over 90% for back-illuminated CCD at certain wavelengths [2, 11].

##### 2.1.1 Internal Quantum Efficiency

---

Internal Quantum Efficiency (IQE) is the ratio of the number of photons that enter the CCD to the number of photons incident on the substrate for a back-illuminated CCD and on the electrodes for a front-illuminated CCD [13]. Its value never reaches the peak value of 100% as there are many losses involved, which are described in the following sections.

### **2.1.2 External Quantum Efficiency**

External Quantum Efficiency (EQE) is the ratio of the number of photo-generated electrons in the CCD to the number of photons incident on the substrate for a back-illuminated CCD and on the electrodes for a front-illuminated CCD [13]. This is generally lower than the IQE for a given device because the electrons have to travel to the depletion region of the CCD to produce an electron-hole pair and they lose energy in this process. The read-out losses also account for the depreciation of the value of the EQE [13].

## **2.2 FACTORS AFFECTING THE QUANTUM EFFICIENCY**

Several factors affect the QE of a CCD. They include numerous effects related to applied potential, the refractive index of the substrate, the crystalline purity of the substrate, operating temperature, doping density, thickness of the substrate, operating modes, radiation damage, etc. Although there are many more such phenomena that alter the QE, there are three major factors which affect the QE substantially. The three factors are the real refractive index, the complex refractive index, and the thickness of the substrate material.

### **2.2.1 Real Refractive Index**

---

The refractive index of a material has two parts, real and complex. The real part of the refractive index symbolised as ‘n’, is commonly used in several equations such as the Snell’s Law equation and to determine the speed of light in a material medium.

The real refractive index is essentially useful in calculating the reflectivity( $R_0$ ) of the substrate surface as per **Eqn. 2.1**.

$$\text{Reflectivity } (R_0) = \left| \frac{n_1 - n_2}{n_1 + n_2} \right|^2 \quad (2.1)$$

Here  $n_1$  refers to the real refractive index at a specific wavelength of the medium from which the light is incident, and  $n_2$  is the real refractive index at a specific wavelength of the medium on which the light is incident.

Reflectivity is the measure of the amount of light of a specific wavelength that will be reflected off the surface of a material [14]. For instance, the reflectivity of 0.45 means that 45% of the incident light will not be able to enter the material’s surface. This parameter should be essentially determined before selecting a material for a CCD. Since a low reflectivity will lead to enhanced performance of a CCD [2].

### 2.2.2 Complex Refractive Index

The complex refractive index of a CCD substrate is an extremely important parameter that is to be contemplated before selecting a material for a CCD. The complex refractive index symbolized as ‘k’, is also referred to as the imaginary refractive index. It is essential for calculating a prominent parameter called the ‘Absorption Coefficient’ using **Eqn. 2.2**.

$$\text{Absorption Coefficient } (\alpha) = \frac{4\pi k}{\lambda} \quad (2.2)$$

Here  $\lambda$  is the wavelength of the incident light. The absorption coefficient can be understood as the distance a photon can travel before it gets completely absorbed inside the material [15]. The larger the value of the absorption coefficient

---

---

of a material for the whole operating wavelength range, the better the material for a photodetector.

### **2.2.3 Thickness of the Substrate Material**

It is very clear from the CCD design explained in the previous chapter that the thickness of the substrate can affect the energies of the photons reaching the depletion region. While travelling inside the substrate, a photon loses energy when it interacts with the electromagnetic fields produced by the atoms and the molecules of the material. To minimize this energy loss, the substrate should be thinned. A CCD substrate cannot be thinned beyond a certain limit as it will introduce interference fringing and make the depletion region thinner, which, in turn, will reduce the performance of a CCD. Hence the thickness of the CCD substrate is set such that its performance is optimised [3].

## **2.3 CONCLUSION**

A CCD's performance is susceptible to many factors. Different studies and methods are adopted to optimise them so that a CCD can deliver the desired results. These methods include experimental testing and simulations. Ensuring that one gets optimum output from a CCD is essential for scientific fields such as astronomy. Astronomical missions (Gaia, James Webb Space Telescope (JWST), etc.) require very high-quality CCDs since they are required to interpret very low-intensity signals and they also do not get a lot of time to observe celestial objects.

---

## CHAPTER 3

### ANTI-REFLECTION (AR) COATINGS

Although silicon is a prominent material in the device-making industry, which is widely used for most semiconductor applications, it has a few drawbacks. One of the major drawbacks of silicon as a CCD material, is reflection loss. To reduce these losses and get the best possible QE of a CCD, AR coatings are applied. An AR coating is a thin layer of a high refractive index material which is applied on the substrate.

#### 3.1 SELECTING THE MATERIALS FOR AR COATINGS

Any random material cannot be used as an AR coating. A material has to be rigorously analysed before it is used as an AR coating. The optical properties of a material govern three parameters, reflectivity, refractive index matching, and absorption coefficient which should be essentially contemplated.

Lesser [11] proposed several materials that can be used as AR coating for astronomical CCDs. Out of those materials hafnium dioxide ( $\text{HfO}_2$ ) is an outstanding material for this purpose. It is currently being used as the AR coating for the Gaia astrometric field (AF) CCDs [16]. Other than  $\text{HfO}_2$ , aluminium oxide ( $\text{Al}_2\text{O}_3$ ), zinc sulphide ( $\text{ZnS}$ ), zirconium dioxide ( $\text{ZrO}_2$ ), and tantalum pentoxide

---

(Ta<sub>2</sub>O<sub>5</sub>) also turned out to be promising materials. The following sections describe how each of these materials satisfies the parameters listed above.

### 3.1.1 Reflectivity

The reflectivity of HfO<sub>2</sub>, Al<sub>2</sub>O<sub>3</sub>, ZnS, ZrO<sub>2</sub>, and Ta<sub>2</sub>O<sub>5</sub> have been determined for the whole wavelength range of the Gaia AF CCDs using **Eqn. 2.1** and are plotted in a comparative graph in **Fig. 3.1**.

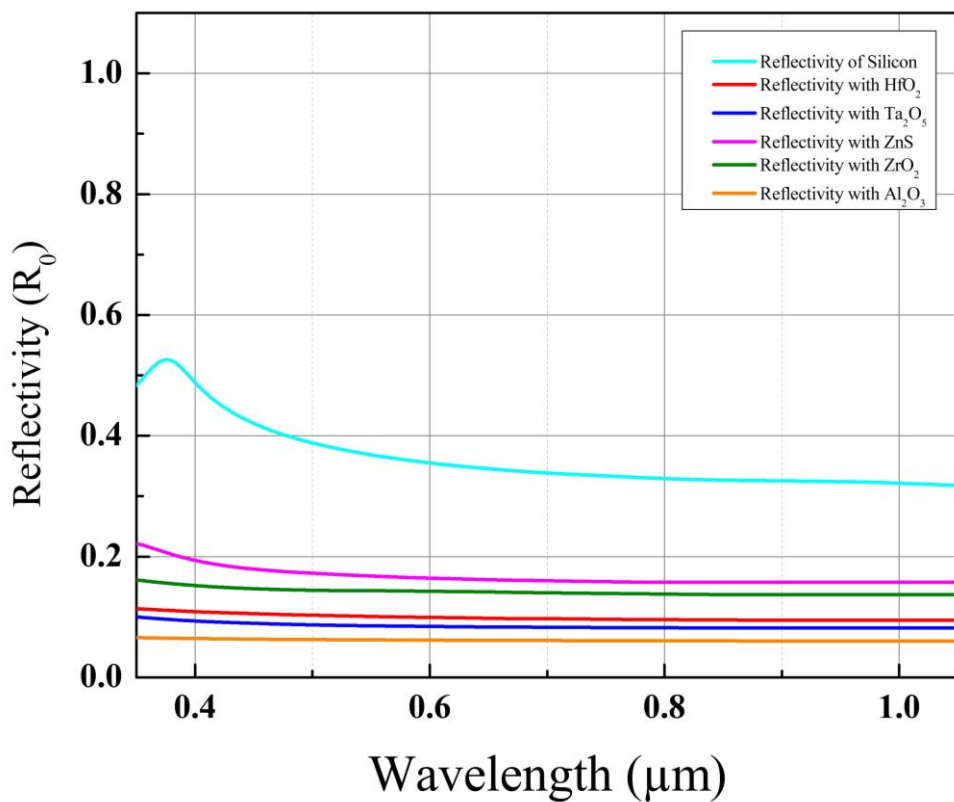


**Fig. 3.1:** Reflectivity of the CCD surface without any AR coating and with different AR coatings

The values of reflectivity reduce effectively after applying AR coatings. It is clearly understandable through **Fig. 3.1** that Al<sub>2</sub>O<sub>3</sub> reduces the reflectivity to the lowest value and ZnS comparatively causes the least reduction in reflectivity of Gaia AF CCD. Ta<sub>2</sub>O<sub>5</sub> decreases the reflectivity to a slightly lower value than HfO<sub>2</sub> while ZrO<sub>2</sub> reduces reflectivity to a slightly higher value than HfO<sub>2</sub>, but the three of them are in close proximity.

---

### 3.1.2 Refractive Index Matching

The matching of the real refractive index of the AR coating material with that of the substrate material is crucial to determine a suitable AR coating for the CCD [11]. In practice, the square root of the refractive index of the substrate material ( $\sqrt{n}$ ) should be in close approximation to the refractive index of the material in consideration at all respective wavelengths within the CCD operation range.

**Fig. 3.2** shows a close matching between the refractive index of  $\text{HfO}_2$  and the square root of the refractive index of silicon in the wavelength range of 330 nm -1050 nm. This suggests that  $\text{HfO}_2$  can prove to be a good AR coating for the Gaia AF CCDs.

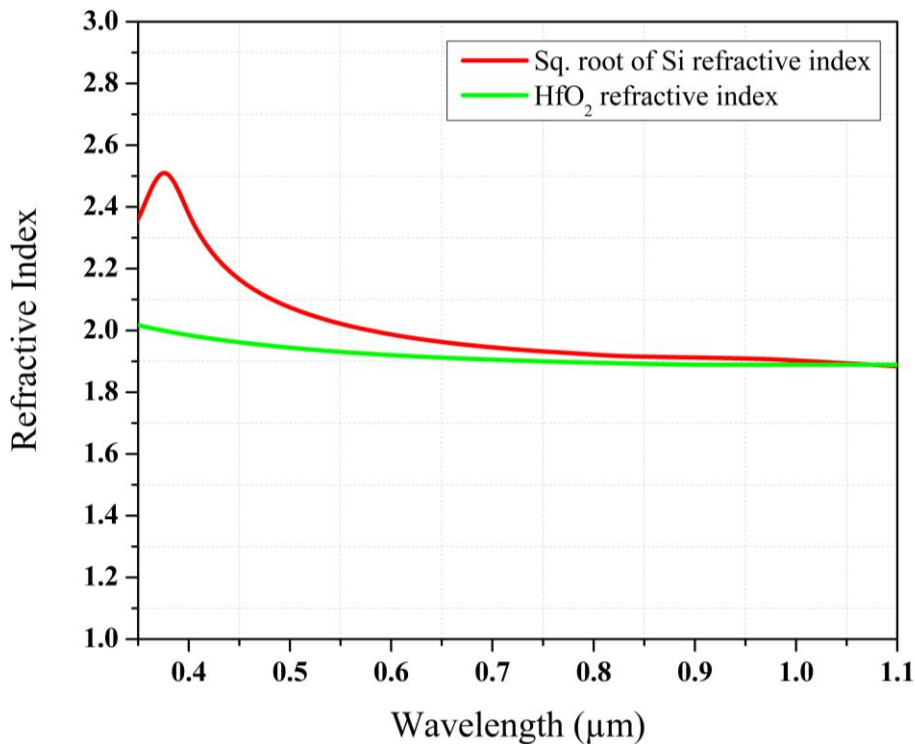


**Fig. 3.2:** Comparison of the refractive index of  $\text{HfO}_2$  with the square root of the refractive index of silicon at different wavelengths

---

**Figs. 3.3, 3.4, 3.5 and 3.6** depict that ZnS and Al<sub>2</sub>O<sub>3</sub> show a relatively poor matching with the square root of the refractive index of silicon in the wavelength range of 330 nm -1050 nm, while ZrO<sub>2</sub> and Ta<sub>2</sub>O<sub>5</sub> exhibit a strong matching. This suggests that HfO<sub>2</sub> can prove to be a good AR coating for the Gaia AF CCDs.

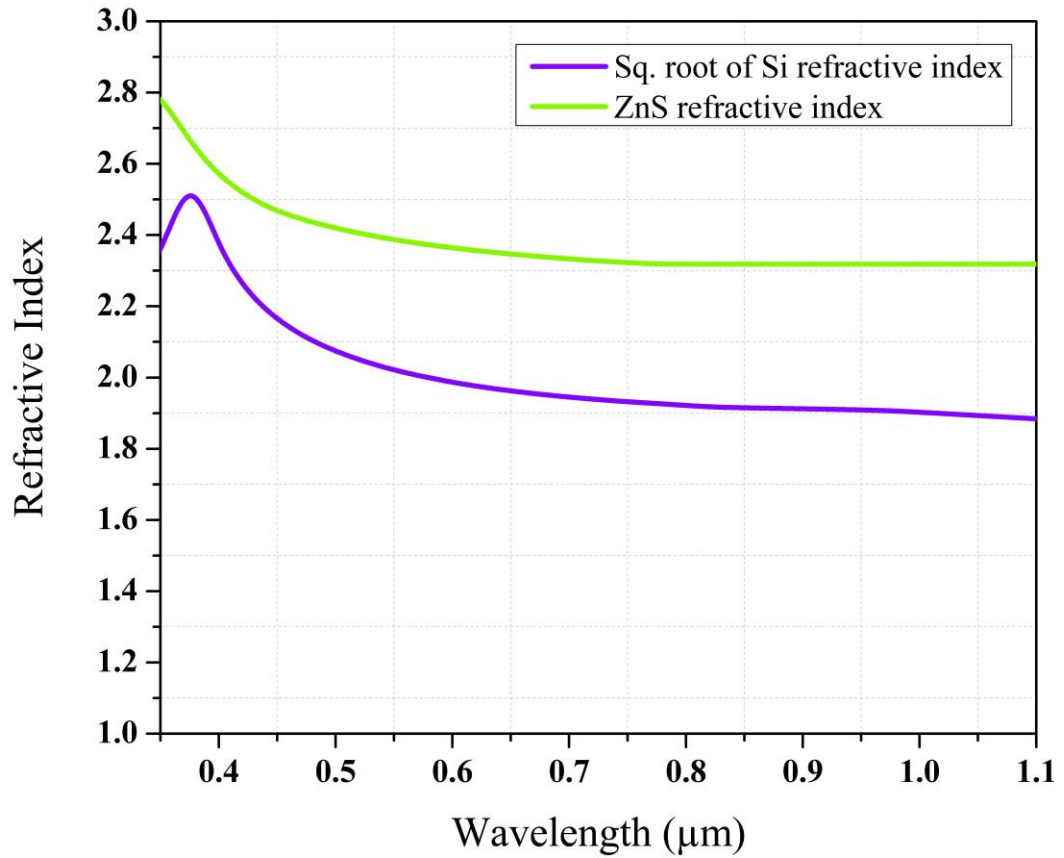


**Fig. 3.3:** Comparison of the refractive index of ZnS with the square root of the refractive index of silicon at different wavelengths



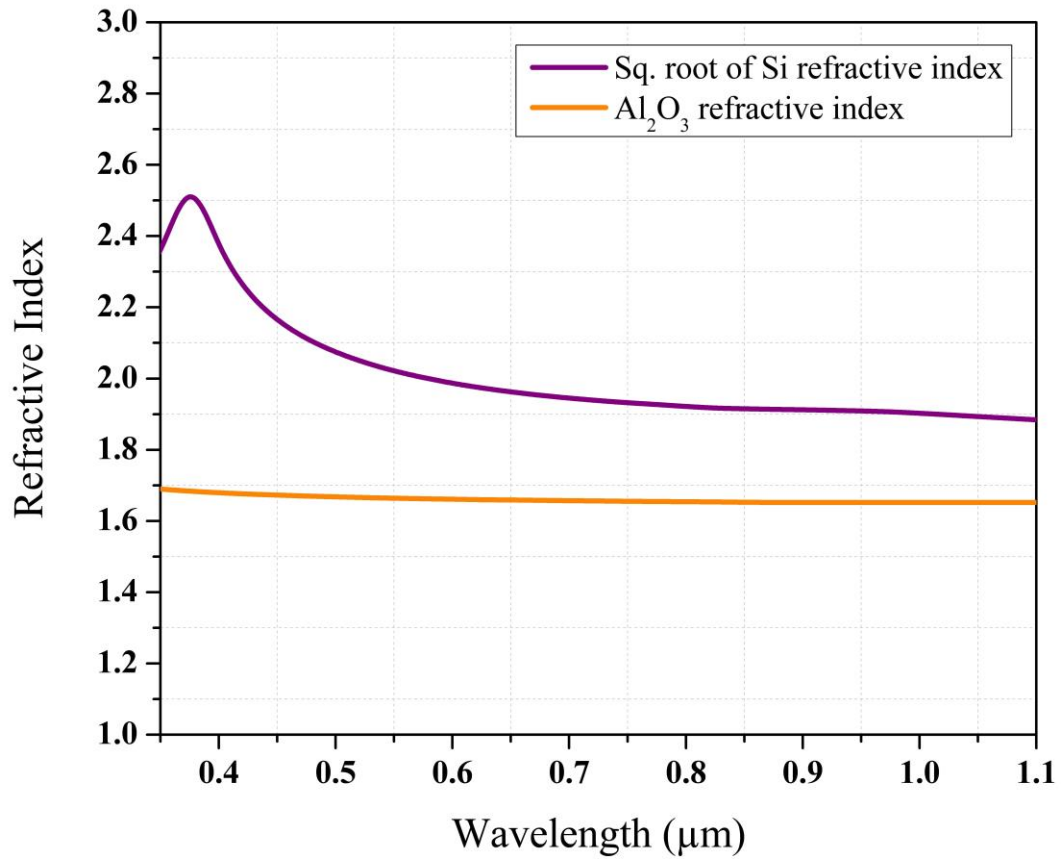


**Fig. 3.4:** Comparison of the refractive index of  $\text{Al}_2\text{O}_3$  with the square root of the refractive index of silicon at different wavelengths

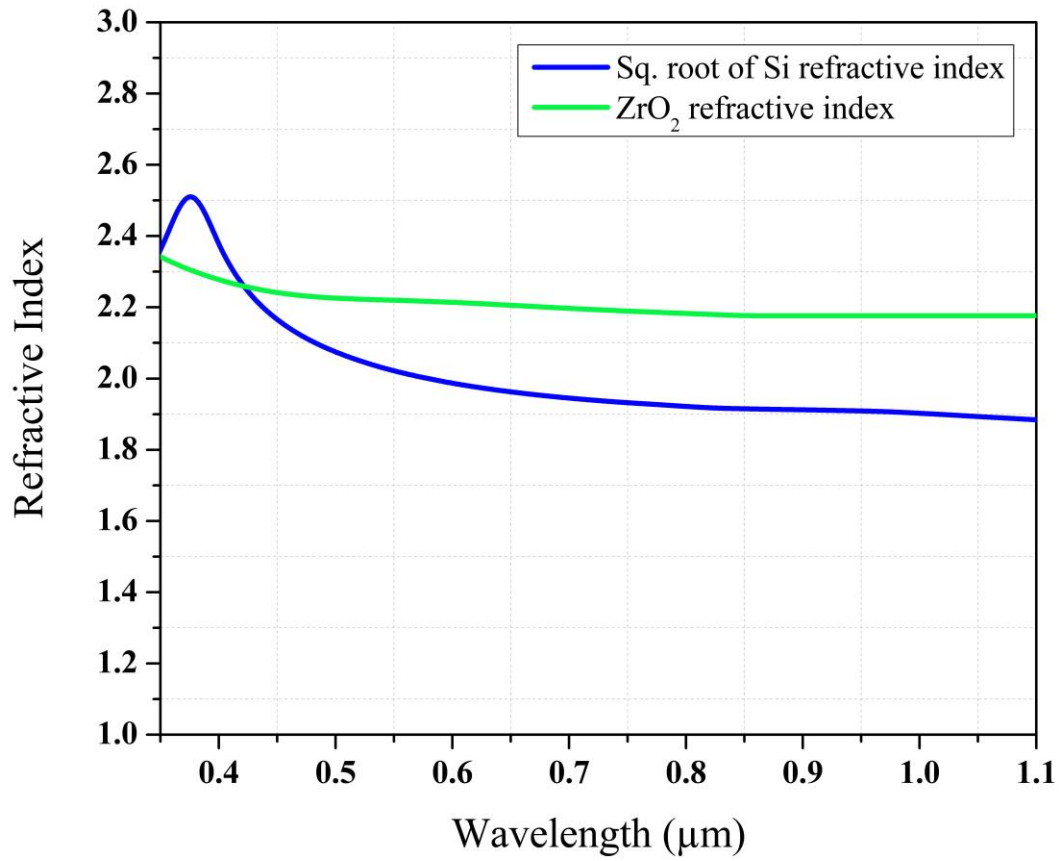


**Fig. 3.5:** Comparison of the refractive index of  $\text{ZrO}_2$  with the square root of the refractive index of silicon at different wavelengths

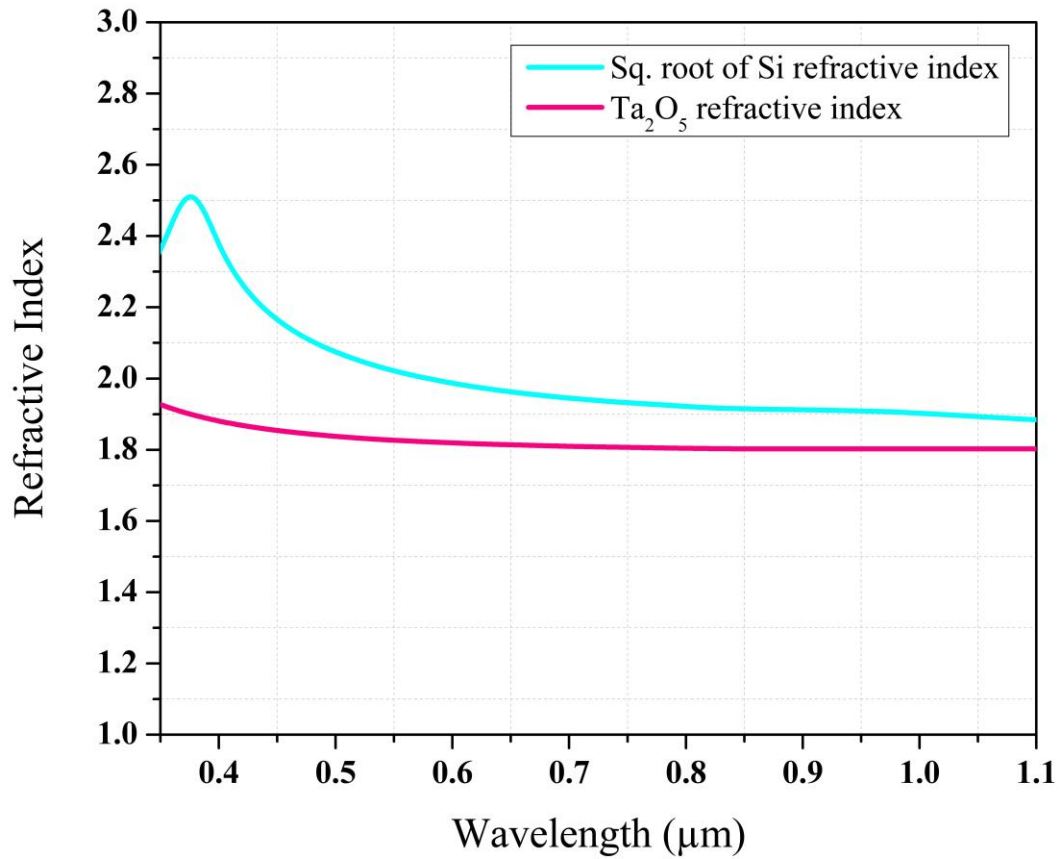


**Fig. 3.6:** Comparison of the refractive index of Ta<sub>2</sub>O<sub>5</sub> with the square root of the refractive index of silicon at different wavelengths

### 3.1.3 Absorption Coefficient

The absorption coefficient of the substrate material plays a substantial role in determining the quantum efficiency of a CCD but is unaffected by an AR coating. This is evident from **Eqn. 2.2**, which shows that it is dependent only upon the imaginary refractive index of the substrate material. It is also depicted in the graphs presented in **Fig. 3.7**.

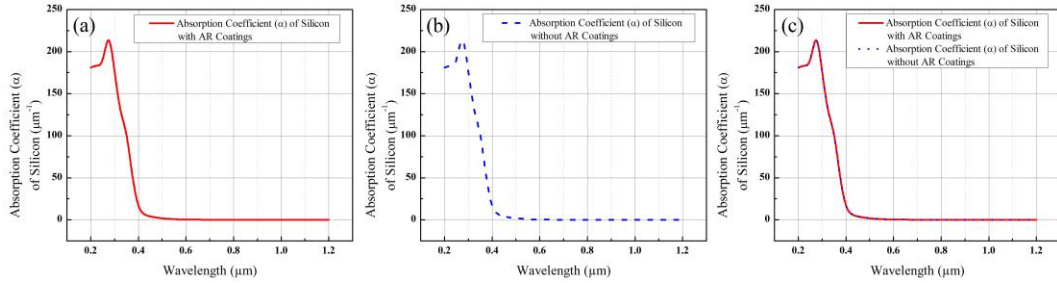


**Fig. 3.7:** The absorption coefficient of silicon **(a)** with AR coatings, **(b)** without AR coatings and **(c)** with and without AR coatings

Hence, in order to obtain a better absorption coefficient for a CCD one must change the substrate material itself.

## 3.2 CONCLUSION

Observing all the above presented data, we can conclude that  $\text{HfO}_2$  satisfies all the conditions required to be a promising AR coating therefore it is currently being used by the Gaia AF CCDs and is providing very good QE. In order to search for alternative AR coating materials that can provide better results, other coatings need to satisfy the above-discussed conditions.

$\text{Al}_2\text{O}_3$  reduces the reflectivity largely, but its refractive index does not match the square root of the refractive index of silicon very well. This suggests that  $\text{Al}_2\text{O}_3$  might give average results.

$\text{ZnS}$  reduces the reflectivity to some extent and its refractive index moderately matches the square root of the refractive index of silicon. It can be deduced that  $\text{ZnS}$  can be used as an AR coating, but it might not give enhanced results as compared to  $\text{HfO}_2$ .

$\text{ZrO}_2$  and  $\text{Ta}_2\text{O}_5$  reduce the reflectivity of silicon substantially and their refractive indices also match the square root of the refractive index of silicon very well, which helps us conclude that they might prove to be good AR coatings and provide improved results as compared to  $\text{HfO}_2$ . They might improve the QE of the Gaia AF CCD and quality of the collected data.

---

## CHAPTER 4

# BENCHMARKING OF THE GAIA ASTROMETRIC FIELD CCD PIXEL STRUCTURE USING SILVACO

The European Space Agency's (ESA) Gaia satellite contains 106 CCDs that are used for many photometric and astrometric measurements. The most abundant CCDs present on the Gaia focal plane are the AF CCDs, which are broadband, back-illuminated detectors [17]. Light is the core of optical astronomy; therefore, it is vital for astrometric devices to collect the maximum possible light. To increase the absorption of incident photons in the CCDs, AR coatings can be applied. To simulate the effects of various AR coatings on the Gaia AF CCDs, SILVACO TCAD software has been used.

SILVACO TCAD software is widely used to model electronic devices so that their performance can be tested and optimised to enhance their performance before they are physically designed. This software is based on Monte Carlo simulations and is used to predict the behaviour of optoelectronic devices in several conditions very well [18, 19].

### 4.1 GAIA PIXEL STRUCTURE

---

To enrich astronomy with more precise measurements, the ESA launched the Gaia Satellite in the L2 orbit in December 2013. Its two telescopes are keeping an eye on millions of stars, galaxies, and solar system objects to produce high-precision astrometric and spectroscopic measurements [17]. The continuous scan gives data sets that are repeatedly reduced to calculate the parallax, position, and proper motion of the celestial objects that are observed by the satellite [20]. The focal plane of the Gaia satellite contains 106 custom-built CCDs. These CCDs were designed and manufactured by e2v technologies, the United Kingdom [16].

Gaia CCDs were fabricated by e2v in three different variants – Astrometric Field (AF), red photometer (RP) and blue photometer (BP); each of these are optimised for different wavelength ranges [21]. The AF CCDs are built using silicon as a substrate with an AR coating which has a maximum photon absorption for light of 650 nm; this CCD has an extensive wavelength detection range of 330-1050 nm [22]. There are 78 AF CCDs on the Gaia Focal plane which are 16  $\mu\text{m}$  thick [20]. The BP and RP are enhanced CCDs that have exceptional sensitivity towards the blue (330-680 nm) and red (640-1050 nm) regions of the light spectrum respectively. 7 BP CCDs present on the Gaia focal plane, have the maximum photon absorption for the light of 360 nm because of its AR coating [20]. Correspondingly, 7 RP CCDs have the maximum photon absorption for light of 750 nm [20]. These CCDs have an image area of 4500 lines  $\times$  1966 columns (here, lines and columns, refer to the rows and columns of the pixels of the CCD respectively) [21]. A schematic diagram of the arrangement of CCDs on the actual Gaia focal plane is shown in **Fig. 4.1**. The detectors are operating in the time delay and integration mode with a period of 982.8  $\mu\text{s}$ , which synchronises their line transfer rate with the satellite rotation rate [20, 21]. In Gaia parlance, line transfer means electrons being transferred in a row of pixels [20].

## Gaia Nominal Focal Plane Design (in approximate agreement with the exact structure)

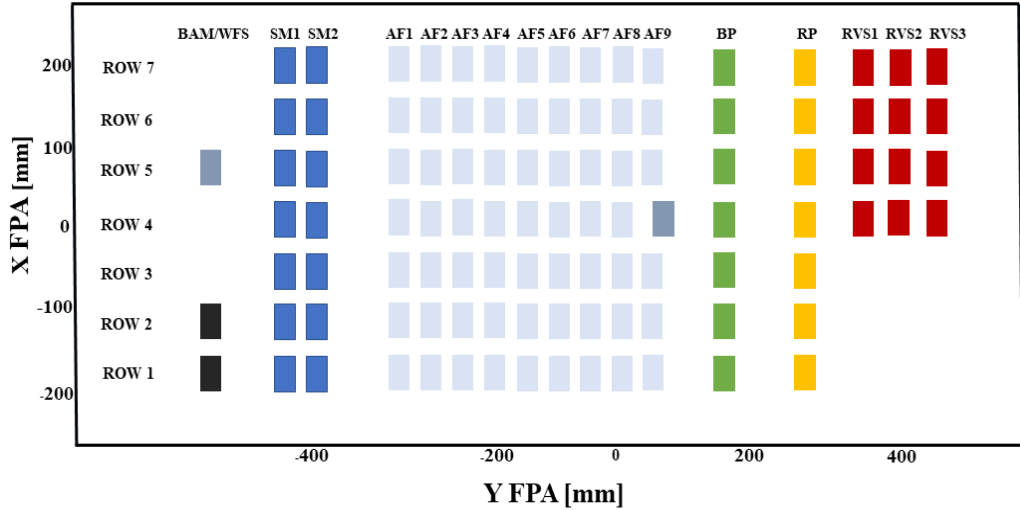


**Fig. 4.1:** The Gaia Focal Plane has 106 CCDs arranged in seven different rows. The red rectangles represent radial velocity spectrometers (RVS). The green and yellow rectangles depict BP and RP respectively, while the grey and black rectangles show wavefront sensors (WFS) and basic angle monitors (BAM) respectively. The light blue rectangles depict the most abundant i.e., AF CCDs and the dark blue rectangles are called sky mappers (SM). The SM and the WFS are also AF CCDs. The RVS and BAM have a construction similar to the RP.

## 4.2 MODELLING USING SILVACO TCAD

SILVACO TCAD is used to simulate several electronic and optical devices. It uses numerical methods for simulations so that the development and optimisation of such devices can be expedited. For simulating the effects of AR coatings on an optoelectronic device, the LUMINOUS and the ATLAS modules of this software can be used.

Since the Gaia AF CCDs are back-illuminated devices, the AR coatings are applied on the backside. Photons are also fired on this side in our simulations.

The operating voltage was set to 10 volts (V) as suggested by [23]. In SILVACO simulations the ratio of available current density ( $J_{\text{available}}$ ) and source current density ( $J_{\text{source}}$ ) gives the IQE of a device. The number of photoelectrons generated in a device can be determined using the electron current density ( $J_n$ ).

For simulating the Gaia AF CCD pixel in SILVACO several structural parameters were required which were derived from [22-25]. The pixel structure of the CCD has three different faces, which is evident from **Fig. 4.2**. We simulated the structure in the across scan (AC) direction in 2D with a pixel size of  $16 \mu\text{m} \times 30 \mu\text{m}$ . The  $16 \mu\text{m}$  thickness of the pixel is subdivided into multiple layers, the details of which are summarised in **Table 4.1**.

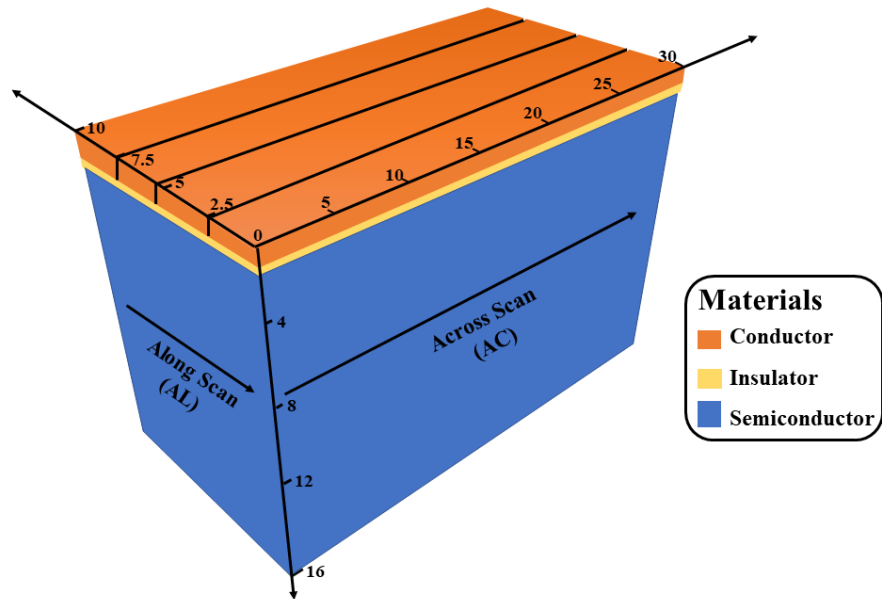


**Fig. 4.2:** Structure of a single pixel of the Gaia AF CCD (all the measurements are in  $\mu\text{m}$ )

**Table 4.1:** The thickness and doping densities of different layers in the AF CCD pixel structure [23].

| S. No. | Material | Type | Thickness ( $\mu\text{m}$ ) | Doping Density ( $\text{cm}^{-3}$ ) |
|--------|----------|------|-----------------------------|-------------------------------------|
|        |          |      |                             |                                     |



---

|   |                         |               |            |                       |
|---|-------------------------|---------------|------------|-----------------------|
| 1 | Polycrystalline silicon | Conductor     | 0-0.5      | 0                     |
| 2 | SiO <sub>2</sub>        | Insulator     | 0.5-0.63   | 0                     |
| 3 | N-type silicon          | Semiconductor | 0.63- 1.17 | $2.65 \times 10^{16}$ |
| 4 | P-type silicon          | Semiconductor | 1.17-16    | $1.3 \times 10^{14}$  |

The length of the BC and the SBC runs from 4.5 to 29  $\mu\text{m}$  in the AC direction [25]. Another prominent feature of Gaia CCDs is an anti-blooming drain (ABD). The ABD, which is present on either side of the pixel in the AC direction is a shielding feature. It prevents the electrons from divulging into the adjacent pixel [24]. To simulate all these interesting features in SILVACO, the whole AF CCD image pixel was modelled with uniform doping as suggested by [23].

The Gaia AF CCDs work at a temperature of 163 K [22] to minimize the dark current, which is attributed to the false positive signals produced in the CCD due to the thermal energy of the electrons [3]. Therefore, to match our theoretical simulations with the experimental results reported by [16], we conducted our simulations at the same temperature.

In order to simulate the CCD pixel structure, the SILVACO ATLAS package uses some constants for the simulated materials that are handled internally. It uses the Monte Carlo method to model the structure. **Table 4.2** compares the experimental values of the constants with the values used during our simulations.

**Table 4.2:** List of theoretical and experimental constants.

| S. No. | Name of the Constant | Theoretical Values used in SILVACO ATLAS | Experimental Values |
|--------|----------------------|--|---------------------|
|        |                      |  |                     |

|    |   |                                      |                           |
|----|---|--------------------------------------|---------------------------|
| 1. | Energy gap of silicon ( $E_g$ )                   | 1.08 eV at 300 K<br>1.11 eV at 163 K | 1.12 eV at 300 K [26]     |
| 2. | Relative Permittivity of silicon ( $\epsilon_r$ ) | 11.8 at 300 K<br>11.8 at 163 K       | 11.66 at 300 K [27]       |
| 3. | Electron Affinity of silicon ( $X$ )              | 4.17 eV at 300 K<br>4.16 eV at 163 K | 4.05 eV at 300 K [28, 29] |
| 4. | Temperature (T)                                   | 163 K                                | 163 K [22]                |

**Fig. 4.3** exhibits the simulated structure of the Gaia AF CCD pixel; the illustration was generated using the Tonyplot tool of the SILVACO software.

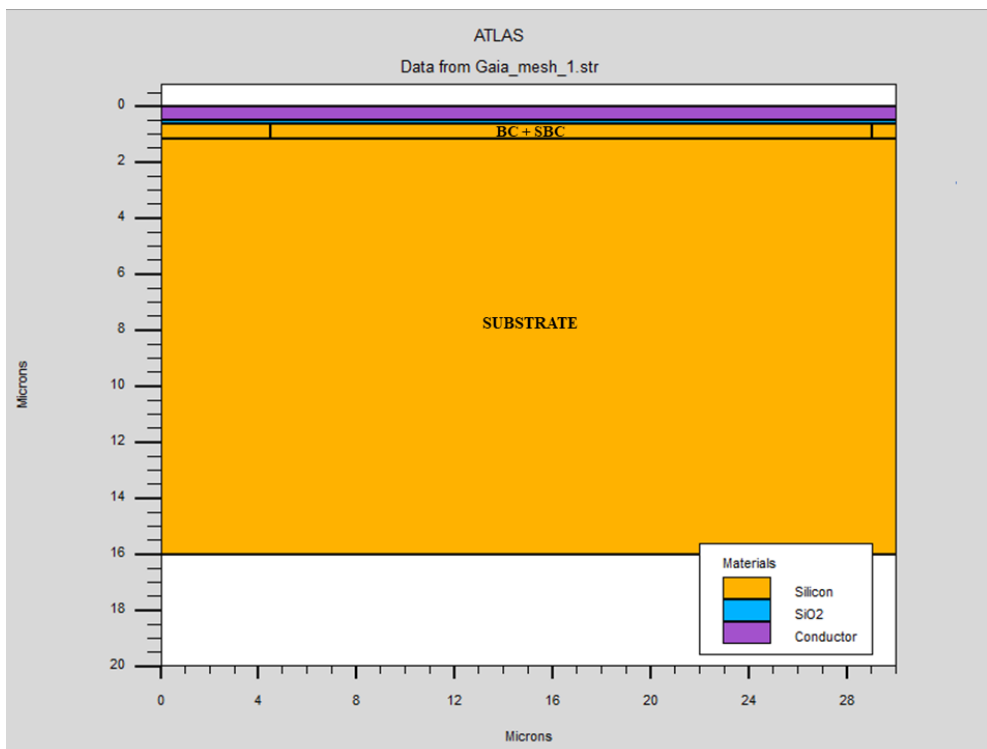


**Fig. 4.3:** The 2D Gaia AF CCD structure in the AC direction as simulated in SILVACO ATLAS

---

### 4.3 COMPARISON WITH REPORTED EXTERNAL QUANTUM EFFICIENCY

We have elucidated the Gaia AF CCD pixel structure used in our simulations, but to test their efficiency the IQE can be used. To begin with, we have focused on single-layer AR coatings that have been applied on the backside of the CCD (substrate side). The thickness of the AR coating is estimated using the quarter wavelength formula (**Eqn. 4.1**).

$$AR\ coating\ thickness = \frac{\lambda}{4n} \quad (4.1)$$

In **Eqn. 4.1**,  $\lambda$  is the wavelength at which the AR coating is centred, i.e., the wavelength at which the AR coating will allow for maximum photon absorption;  $n$  is the refractive index of the AR coating material at the wavelength  $\lambda$  [11]. The SOPRA database of the SILVACO ATLAS software was tremendously helpful in allowing us to include the refractive indices of the AR coatings.

While simulating the pixel structure with the HfO<sub>2</sub> AR coating, the **Eqn. 4.1** deduces the thickness of the coating as 0.085  $\mu\text{m}$ . We identified the EQE for this setup to benchmark our simulations against the previously published EQE values by [16]. The simulation results are comparable to the experimental results, which can be visualised in **Fig. 4.4**. Any differences in the values of EQE might be because of the absence of ABD in our structure as the parameters required for its simulations were not published in the current literature.

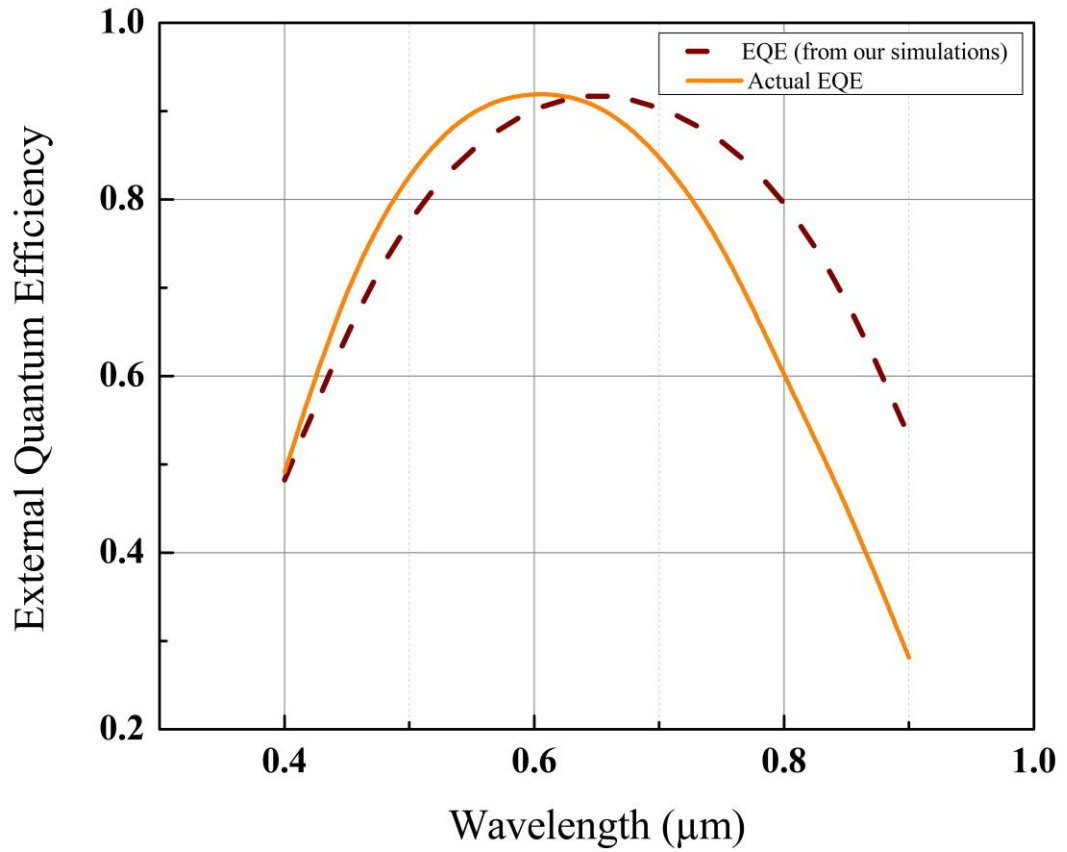


**Fig 4.4:** Comparison of the actual EQE of the Gaia AF CCDs and the EQE obtained from the simulations

#### 4.4 CONCLUSION

Gaia has provided astronomers with a better eye to view our sparkling galaxy. This would not have been possible without the AF CCDs. We simulated their structure using SILVACO TCAD. The results of the simulations matched with the previously published literature by [16]. This allowed the benchmarking of the simulated model and proved to be a base for further testing to improve the QE of the Gaia AF CCDs.

---

## CHAPTER 5

# STUDY OF THE QE OF THE GAIA AF CCD PIXEL MODEL WITH SEVERAL AR COATINGS

The importance of AR coatings for the Gaia AF CCD is unquestionable. The currently used HfO<sub>2</sub> and other materials for coatings have been investigated using the SILVACO TCAD software. The QE of the Gaia AF CCDs with different AR coatings has been determined for the whole spectral range.

### 5.1 WITH HAFNIUM DIOXIDE

On calculating the IQE for the Gaia AF CCD without applying any AR coating, it was discovered that they have a maximum IQE of 0.65 at the wavelength of 0.7  $\mu\text{m}$ . Comparing the IQE of the CCDs with and without the HfO<sub>2</sub> coating, we clearly observe an average increment of about 37.2% in the whole wavelength range. **Fig. 5.1** conveys this increment graphically.

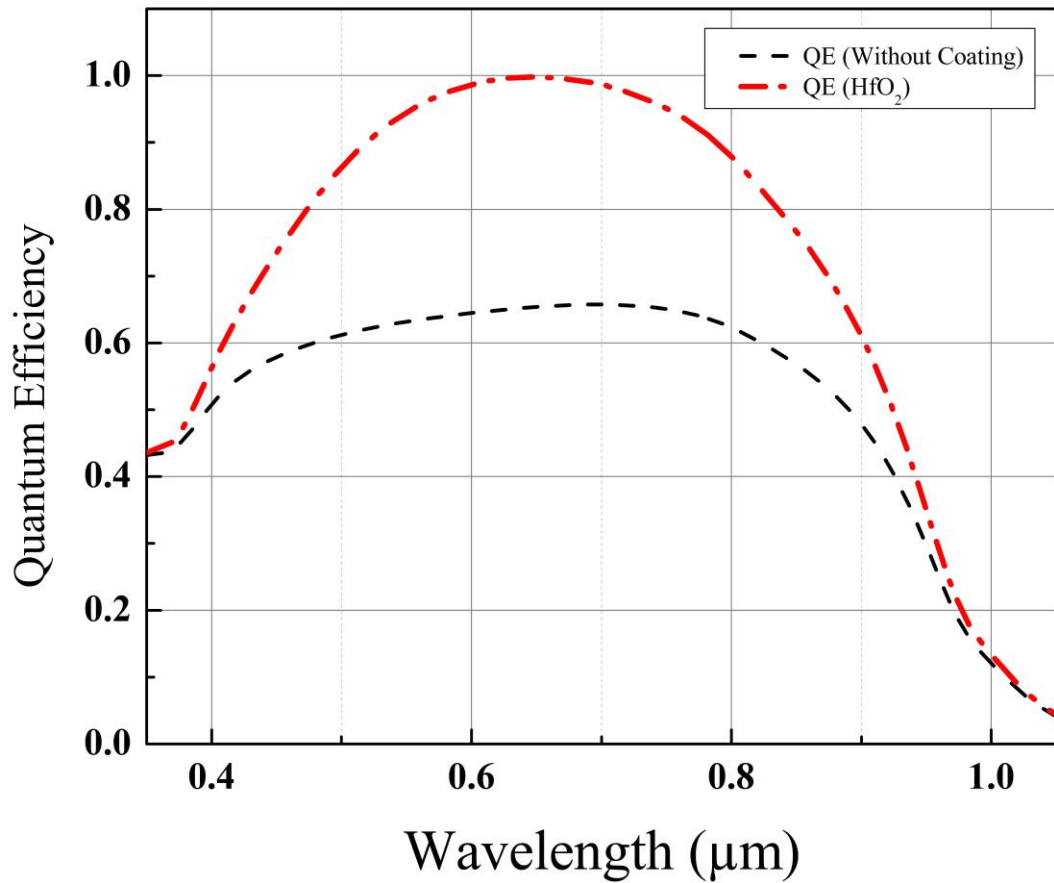


**Fig 5.1:** QE of the Gaia AF CCD without and with an HfO<sub>2</sub> AR coating

## 5.2 WITH ZINC SULPHIDE

As per our study of AR coating materials, we choose four AR coatings to test our device. ZnS being one of them. Application of 0.069 μm thick single layer coating of ZnS, centred at 0.65 μm, unfolds that it is not very suitable for our device. The IQE curve in **Fig. 5.2** outlines that there is an average decrement of approximately 3.5% when studied parallel to the Gaia AF CCD with a HfO<sub>2</sub> AR coating in the whole range.

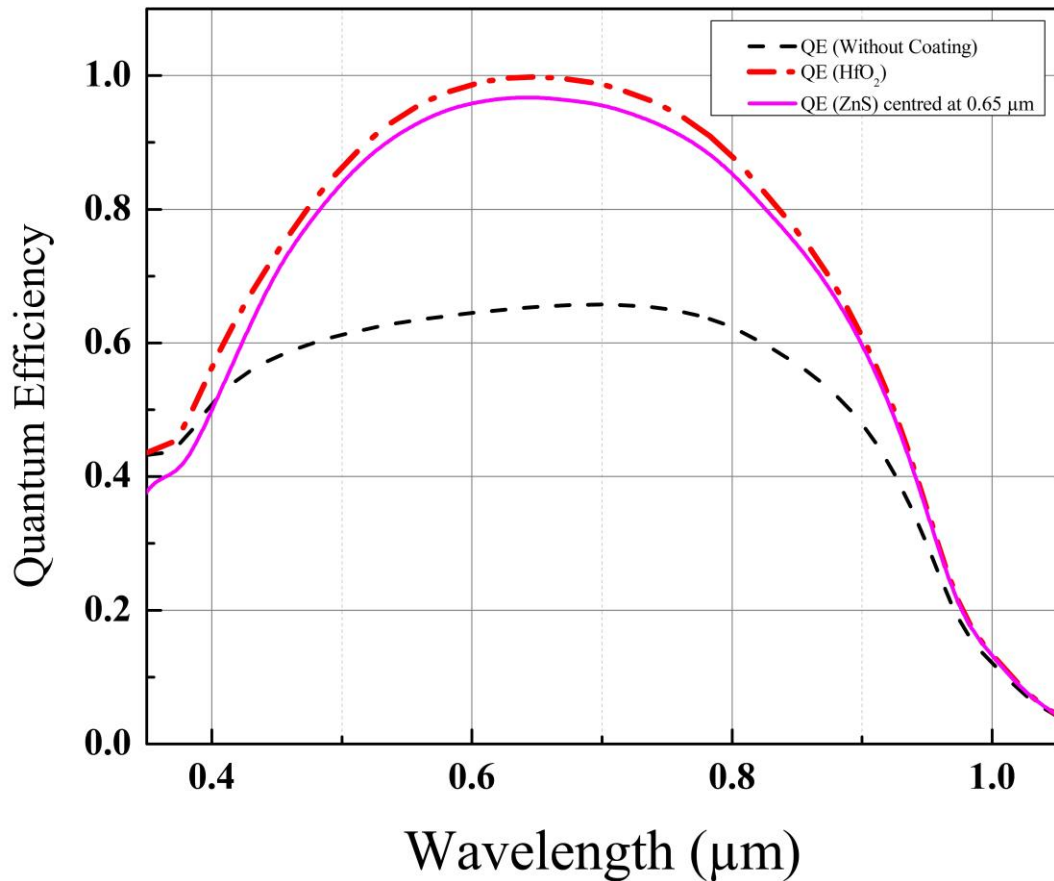


**Fig 5.2:** QE of the Gaia AF CCD without an AR coating, with an HfO<sub>2</sub> AR coating, and with a ZnS AR coating

### 5.3 WITH ALUMINIUM OXIDE

Our next choice was Al<sub>2</sub>O<sub>3</sub> therefore we applied a single layer of it with a thickness of about 0.098 μm (calculated as per **Eqn. 4.1**), centred at 0.65 μm. The Gaia AF CCD with HfO<sub>2</sub> AR coating still provides better results for most wavelengths as compared to Al<sub>2</sub>O<sub>3</sub>. It is also observed that Al<sub>2</sub>O<sub>3</sub> coating provides an average improvement in IQE of about 1.3% in the 0.35 μm to 0.425 μm range and an average decrement of about 1.9% in the rest of the wavelength range. These results are compiled in the graph presented in **Fig. 5.3**.

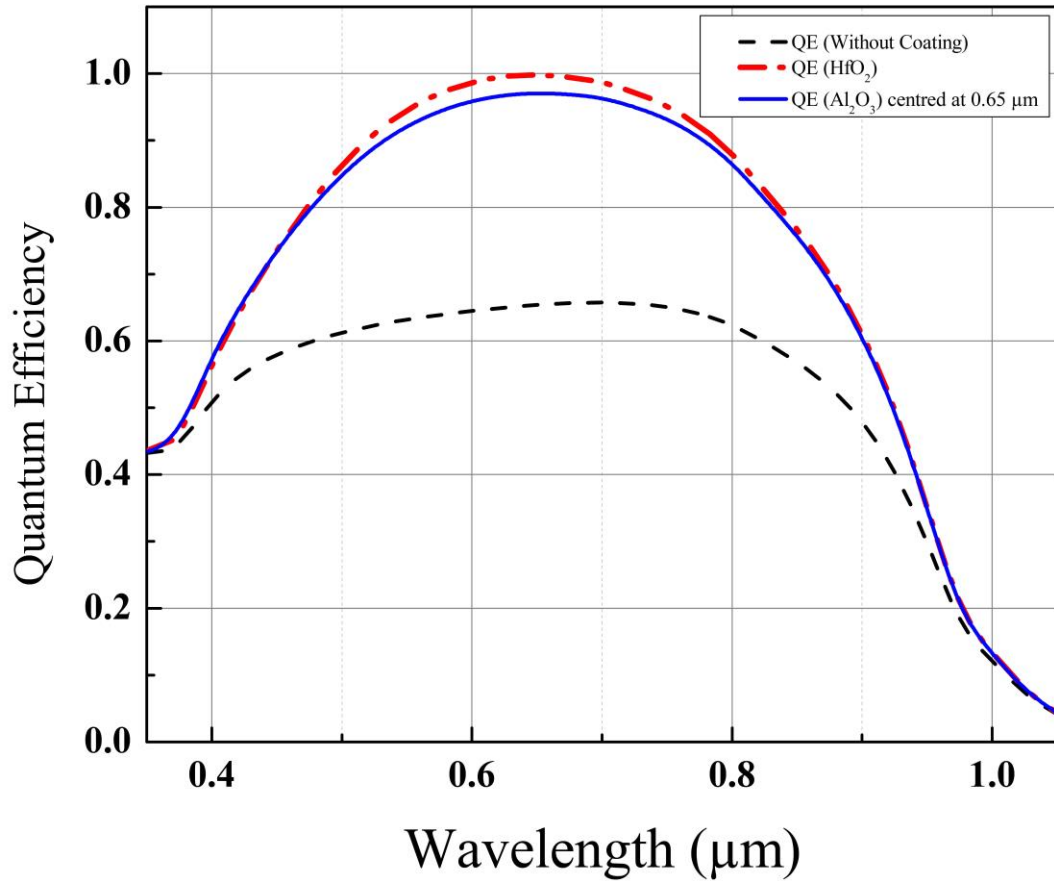


**Fig 5.3:** QE of the Gaia AF CCD without an AR coating, with an HfO<sub>2</sub> AR coating, and with an Al<sub>2</sub>O<sub>3</sub> AR coating

#### 5.4 WITH ZIRCONIUM DIOXIDE

The next alternative that we analysed was a single-layer coating of ZrO<sub>2</sub> centred at 0.65 μm. The thickness of the coating was set as per **Eqn. 4.1** close to 0.073 μm. After observing the graphical data presented in **Fig. 5.4**, we infer that there is an average increment in the IQE of around 0.8% in the range of 0.4 μm to 0.525 μm when analysed with the IQE values when HfO<sub>2</sub> coating was applied. For the rest of the wavelengths, the AR coating of HfO<sub>2</sub> offers an average increment of almost 1.1%, when compared to ZrO<sub>2</sub>.



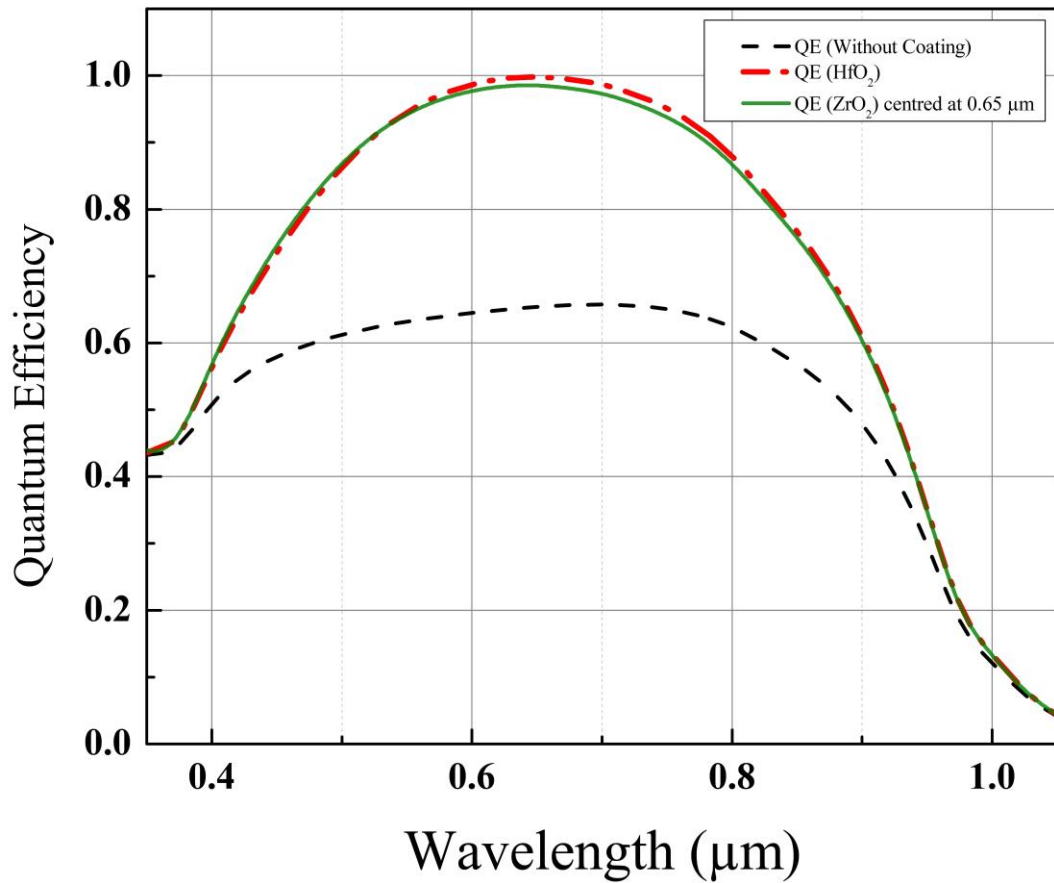


**Fig 5.4:** QE of the Gaia AF CCD without an AR coating, with an HfO<sub>2</sub> AR coating, and with an ZrO<sub>2</sub> AR coating centred at 0.65 μm

Inspired by the improvements shown by ZrO<sub>2</sub>, we adjusted its thickness to an approximate value of 0.071 μm, which allows for a peak absorbance of the light of wavelength 0.625 μm. This experimentation of ours yields an average increment of nearly 4% for the wavelength range of 0.375 μm to 0.575 μm when compared with HfO<sub>2</sub>. with an average compromise of around 2% in the wavelength range of 0.575 μm to 1.05 μm. This data is visualised in **Fig. 5.5**.

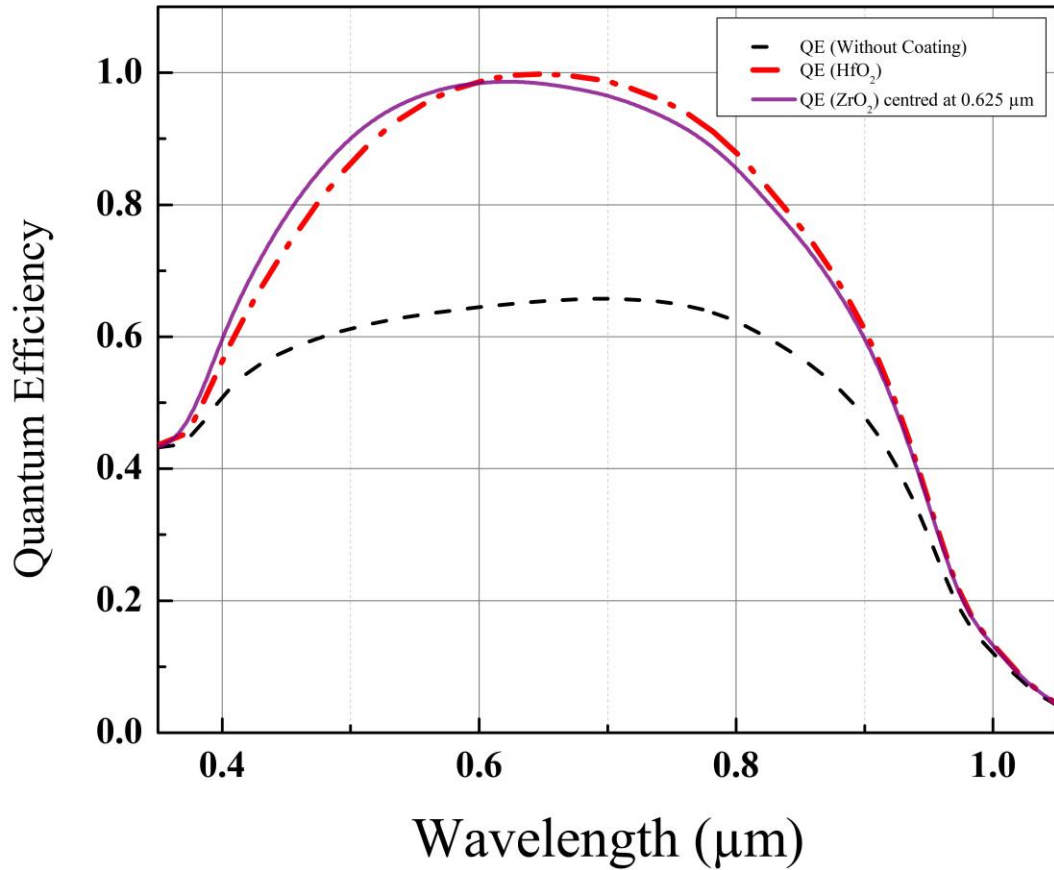


**Fig 5.5:** QE of the Gaia AF CCD without an AR coating, with an HfO<sub>2</sub> AR coating, and with an ZrO<sub>2</sub> AR coating centred at 0.625 μm

## 5.5 WITH TANTALUM PENTOXIDE

We concluded our studies with Ta<sub>2</sub>O<sub>5</sub> which is a promising AR coating. A single layer of Ta<sub>2</sub>O<sub>5</sub>, centred at 0.65 μm with a thickness of approximately 0.09 μm (calculated using **Eqn. 4.1**) permits almost the same performance as HfO<sub>2</sub>. It is evident from **Fig. 5.6** that the two curves virtually overlap each other in the whole range. We did not obtain such promising results for any other AR coating. Hence, to improve the IQE in the low wavelength region, we deposited a 0.086 μm thick layer of Ta<sub>2</sub>O<sub>5</sub> to centre the AR coating at 0.625 μm. The IQE of the Gaia AF CCDs with an AR coating of Ta<sub>2</sub>O<sub>5</sub> shows an average increment of about 2.8% as compared to the CCDs with HfO<sub>2</sub> AR coating in the wavelength range of 0.375 μm

---

to 0.6  $\mu\text{m}$ . There is an average decrease of around 1.2% in the IQE of the wavelengths ranging from 0.6  $\mu\text{m}$  to 1.05  $\mu\text{m}$  which is clearly evident in **Fig. 5.7**.

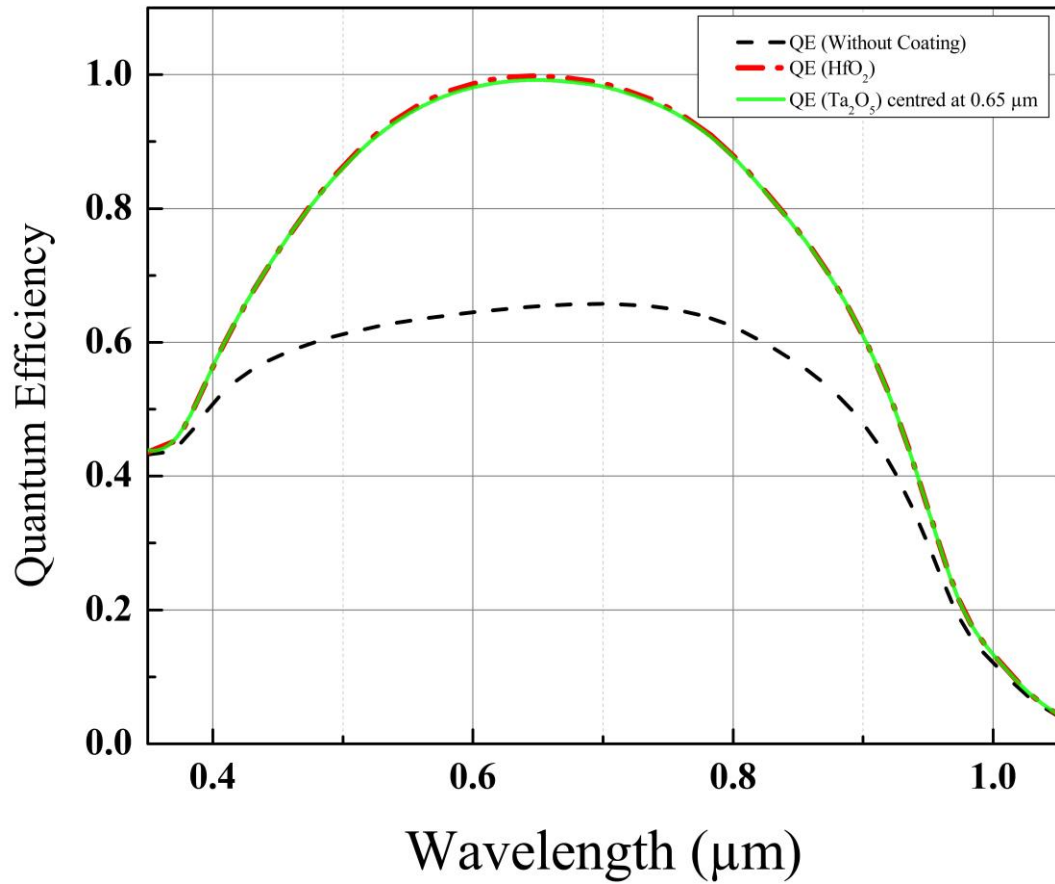


**Fig 5.6:** QE of the Gaia AF CCD without an AR coating, with an HfO<sub>2</sub> AR coating, and with an Ta<sub>2</sub>O<sub>5</sub> AR coating centred at 0.65  $\mu\text{m}$

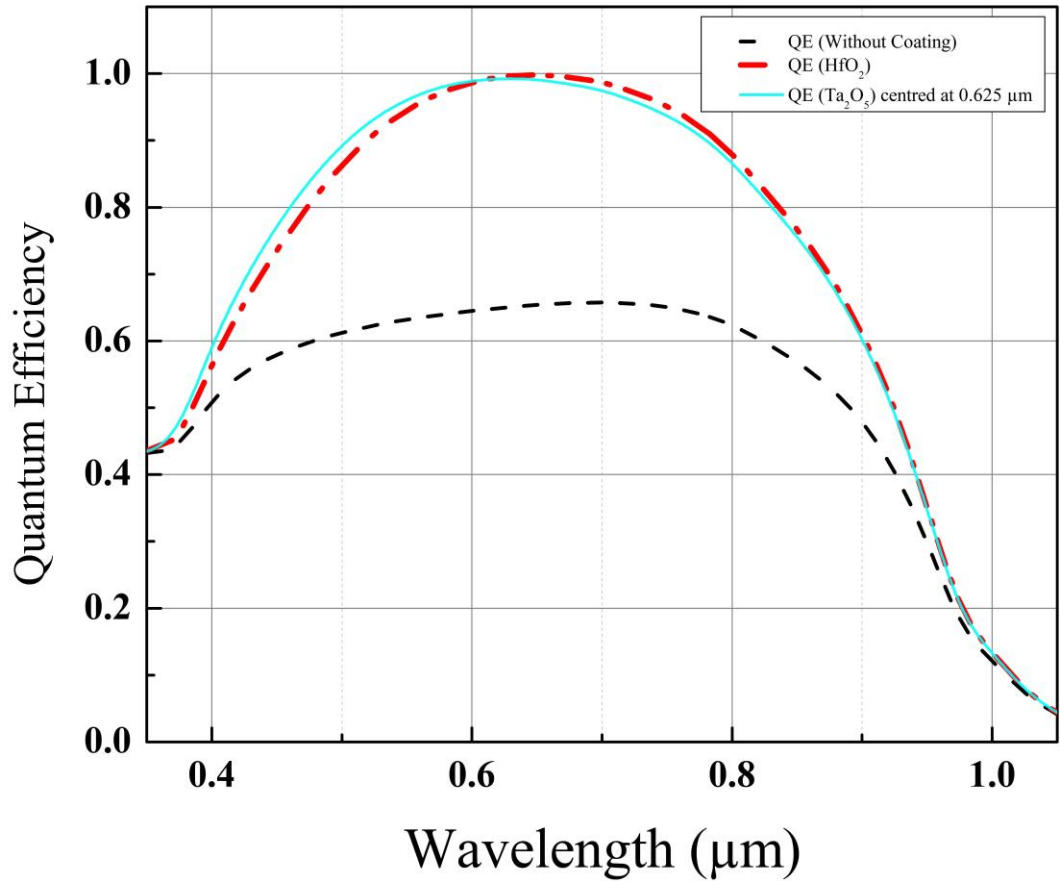


**Fig 5.7:** QE of the Gaia AF CCD without an AR coating, with an HfO<sub>2</sub> AR coating, and with an Ta<sub>2</sub>O<sub>5</sub> AR coating centred at 0.625 μm

## 5.6 CONCLUSION

A comparative study has been drawn to analyse which AR coating best suits the Gaia AF CCDs. It is observed that a single layer coating of ZrO<sub>2</sub> and Ta<sub>2</sub>O<sub>5</sub> gives similar or better results as compared to HfO<sub>2</sub> for most wavelengths lying in Gaia's AF CCD range (330-1050 nm) [22]. **Table 5.1** summarises the comparison among the IQE of CCDs for different AR coatings.

**Table 5.1:** Percentage increment and decrement in the QE of the Gaia AF CCD with different AR coatings as compared to the HfO<sub>2</sub> AR coating.

| S. N. | AR Coatings  | Wavelength Range ( $\mu\text{m}$ ) | Percentage Increment/<br>Decrement<br>in the IQE                      | Average Increment/<br>Decrement<br>in the IQE                 |
|-------|--|------------------------------------|---|---|
| 1.    | HfO <sub>2</sub>   | 0.33 – 1.05                        | Increment (2.6% to 53.3%) as compared to a CCD without any AR coating | Increment (37.2%) as compared to a CCD without any AR coating |
| 2.    | ZnS<br>(centred at 0.65 $\mu\text{m}$ )                            | 0.35 – 1.05                        | Decrement (0.3% to 12.2%) as compared to HfO <sub>2</sub>             | Decrement (3.5%) as compared to HfO <sub>2</sub>              |
| 3.    | Al <sub>2</sub> O <sub>3</sub><br>(centred at 0.65 $\mu\text{m}$ ) | 0.35 – 0.425                       | Increment (0.1% to 2.3%) as compared to HfO <sub>2</sub>              | Increment (1.3%) as compared to HfO <sub>2</sub>              |
|       |  | 0.425-1.05                         | Decrement (0.09% to 2.8%) as compared to HfO <sub>2</sub>             | Decrement (1.9%) as compared to HfO <sub>2</sub>              |
| 4.    | ZrO <sub>2</sub><br>(centred at 0.65 $\mu\text{m}$ )               | 0.4 – 0.525                        | Increment (0.04% to 1.35%) as compared to HfO <sub>2</sub>            | Increment (0.8%) as compared to HfO <sub>2</sub>              |
|       |  | 0.525 -1.05                        | Decrement (0.19% to 1.4%) as compared to HfO <sub>2</sub>             | Decrement (1.1%) as compared to HfO <sub>2</sub>              |

|    |  |                  |  |   |
|----|--|------------------|--|---|
| 5. | ZrO <sub>2</sub><br>(centred<br>at 0.625<br>μm)                  | 0.375 –<br>0.575 | Increment (0.63% to<br>6.85%) as compared<br>to HfO <sub>2</sub> | Increment (4%)<br>as compared to<br>HfO <sub>2</sub>      |
|    |  | 0.575 – 1.05     | Decrement (0.38% to<br>2.72%) as compared<br>to HfO <sub>2</sub> | Decrement (2%) as<br>compared to HfO <sub>2</sub>         |
| 6. | Ta <sub>2</sub> O <sub>5</sub><br>(centred<br>at 0.65<br>μm)     | 0.35 – 0.9       | Decrement (0.64%<br>and less)<br>as compared to HfO <sub>2</sub> | No prominent<br>change as compared<br>to HfO <sub>2</sub> |
|    |  | 0.9 - 1.05       | Increment (0.04%<br>and less) as compared<br>to HfO <sub>2</sub> | No prominent<br>change as compared<br>to HfO <sub>2</sub> |
| 7. | Ta <sub>2</sub> O <sub>5</sub><br>(centred<br>at<br>0.625<br>μm) | 0.375 – 0.6      | Increment (0.17% to<br>5.15%) as compared<br>to HfO <sub>2</sub> | Increment (2.8%) as<br>compared to HfO <sub>2</sub>       |
|    |  | 0.6 – 1.05       | Decrement (0.19% to<br>1.57%) as compared<br>to HfO <sub>2</sub> | Decrement (1.2%)<br>as compared to<br>HfO <sub>2</sub>    |

---

## CHAPTER 6

# ANALYSIS OF GALLIUM NITRIDE AS AN ALTERNATIVE TO SILICON FOR ASTRONOMICAL CCDs

The importance of radiation in astronomy is paramount. It is the one single physical quantity that governs the oldest science. It is advertently clear from the above studies that even with suitable AR coatings a silicon detector is unsuitable for low ( $< 500$  nm) and high ( $> 800$  nm) wavelength regions of the operational spectrum of the Gaia AF CCDs.

There can be several reasons for this, but the two main factors responsible for silicon's behaviour in these regions are its high reflectivity and low absorption coefficient.

It has been described in the previous chapters that in order to have a better absorption coefficient for the CCD the material from which the CCD substrate is made has to be deeply deliberated over. The properties of the material chosen should be such that it offers low reflectivity and a high absorption coefficient, while also performing electrically well.

### **6.1 IMPORTANCE OF IMAGINARY REFRACTIVE INDEX**

---

The absorption coefficient is perhaps the most important of the parameters defined in **Chapter 2** for the quantum efficiency of a CCD. The reason for this can be understood from the graphs in **Fig. 6.1**.

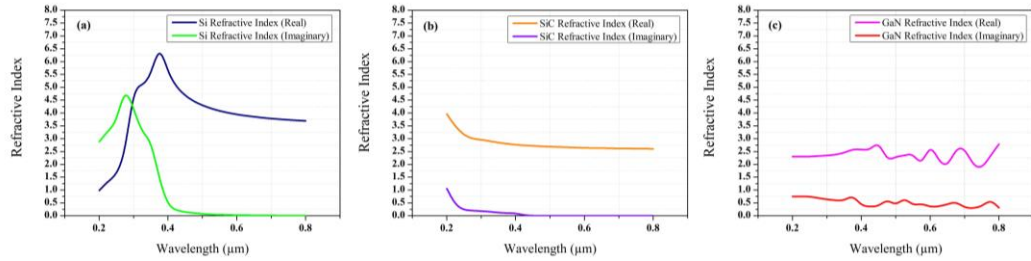


**Fig. 6.1:** The real ( $n$ ) and imaginary refractive indices ( $k$ ) of (a) silicon, (b) silicon carbide (SiC), and (c) gallium nitride (GaN) in the wavelength range of 0.2  $\mu\text{m}$  to 0.8  $\mu\text{m}$ .

SILVACO TCAD’s SOPRA database has been used for the plots in **Fig. 6.1** [18, 19]. It can be comprehended from **Fig. 6.1 (a)** that the value of  $k$  decreases sharply for silicon until about 0.4  $\mu\text{m}$  and assumes an extremely small value thereafter. This implies that silicon has a very small value of absorption coefficient after 0.4  $\mu\text{m}$ . The absorption coefficient of a material at a specific wavelength can be calculated as per **Eqn. 2.2**, for silicon they have been calculated and are presented in **Fig. 3.7**.

It can be observed in **Fig. 6.1 (a), (b), and (c)** that along with a small absorption coefficient the reflectivity of silicon will be quite high above 0.4  $\mu\text{m}$  when compared to SiC and GaN because of its high value of  $n$ . For the wavelength range below 0.4  $\mu\text{m}$  until 0.2  $\mu\text{m}$  the value of  $n$  for silicon is substantially higher in contrast to SiC and GaN. This means that silicon will provide a higher reflectivity in this range in comparison to SiC and GaN. The average reflectivity of silicon in the wavelength range of 0.2  $\mu\text{m}$  to 0.45  $\mu\text{m}$  is about 47 %. Furthermore, due to a large variation in the real refractive index curve in **Fig. 6.1 (a)** in this range, it is hard to find a suitable AR coating to reduce such reflectivity, as refractive index matching is essential for them as described in **Section 3.1.2**. Hence, silicon does not prove to be a very good photodetector in high ( $> 800 \text{ nm}$ ) and low ( $< 500 \text{ nm}$ ) wavelength ranges.



---

A similar trend for the complex refractive index of SiC can be observed in **Fig. 6.1 (b)**, but with much less values of  $n$  in the wavelength range of  $0.2 \mu\text{m} - 0.4 \mu\text{m}$  in comparison to silicon. This makes SiC highly suitable for low-wavelength photodetectors [30-34], but for broadband detectors like the Gaia AF CCDs, these desirable properties are required for a much larger wavelength range. This can be seen for GaN in **Fig. 6.1 (c)**.

## **6.2 SUITABILITY OF GaN FOR BROADBAND ASTRONOMICAL CCDs**

As evident from **Fig. 6.1 (c)** and the above discussion, the suitability of GaN for broadband astronomical CCDs can be attributed to its comparatively low values of  $n$  and higher values of  $k$  in a broadband wavelength range. It can be expected from GaN that it will help to achieve low reflectivity and a high absorption coefficient in the whole operational wavelength range of the Gaia AF CCDs. It also has superior conductivity when compared to silicon [35].

The major reason why GaN is only used for low wavelength applications is because of its high bandgap and radiation hardness properties [35-41]. The bandgap of GaN at room temperature is about 3.3 eV [26]. Compared to silicon's bandgap of about 1.1 eV it is quite large [26]. For a broadband CCD a bandgap near to or less than silicon's bandgap is required, so that photogeneration can take place. To reduce the bandgap of GaN for its use in broadband astronomical CCDs, the bandgap narrowing property of a semiconductor can be used, which is directly related to the doping concentration [35, 39].

## **6.3 SIMULATION AND CALCULATIONS FOR THE GaN CCD PIXEL STRUCTURE**

To simulate the GaN CCD pixel structure and compare its performance with the silicon Gaia AF CCD pixel structure the dimensions of both models have been set to the same values. The Gaia AF CCD pixel structure parameters used for

---

---

the simulations are mentioned in **Table 4.1**. The only differences between the two models are that for the GaN structure, the doping values have been varied and GaN is used instead of silicon for the n-type and p-type layers, other parameters such as temperature, operating potential, etc. remain the same for the simulation of both the models.

The n-type doping concentration used for GaN is  $1.00 \times 10^{21} \text{ cm}^{-3}$ , and the p-type doping concentration has been set to  $8.9 \times 10^{19} \text{ cm}^{-3}$ . These values have been carefully set to cause sufficient band gap narrowing. The narrowed bandgap values of the GaN model for n-type and p-type substrates have been calculated using the equations mentioned in [18, 19, 35, 39].

#### **6.4 COMPARISON OF THE GaN CCD MODEL WITH THE GAIA AF CCD MODEL**

The first step to propose GaN as an alternative to silicon for broadband astronomical CCDs is to test and compare their electrical performance. The potential profiles of the silicon pixel and the GaN pixel models have been presented in **Figs. 6.2** and **6.3** respectively. The Tonyplot tool of the SILVACO software has been used to generate them.

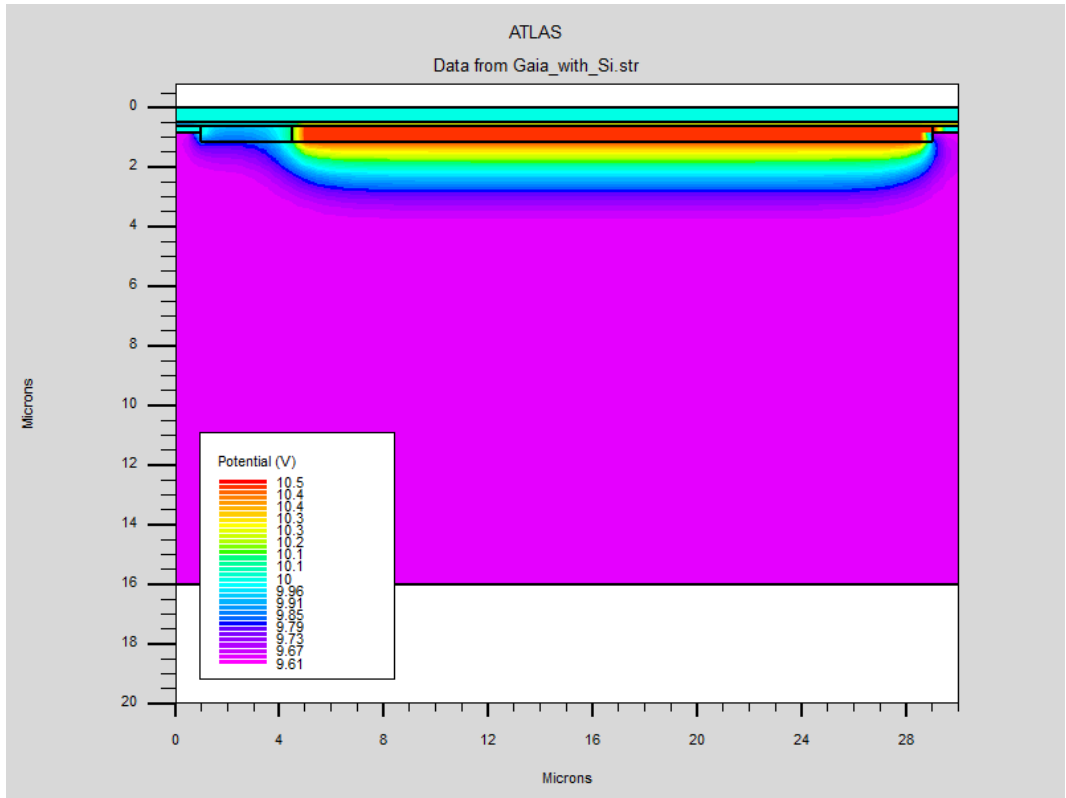
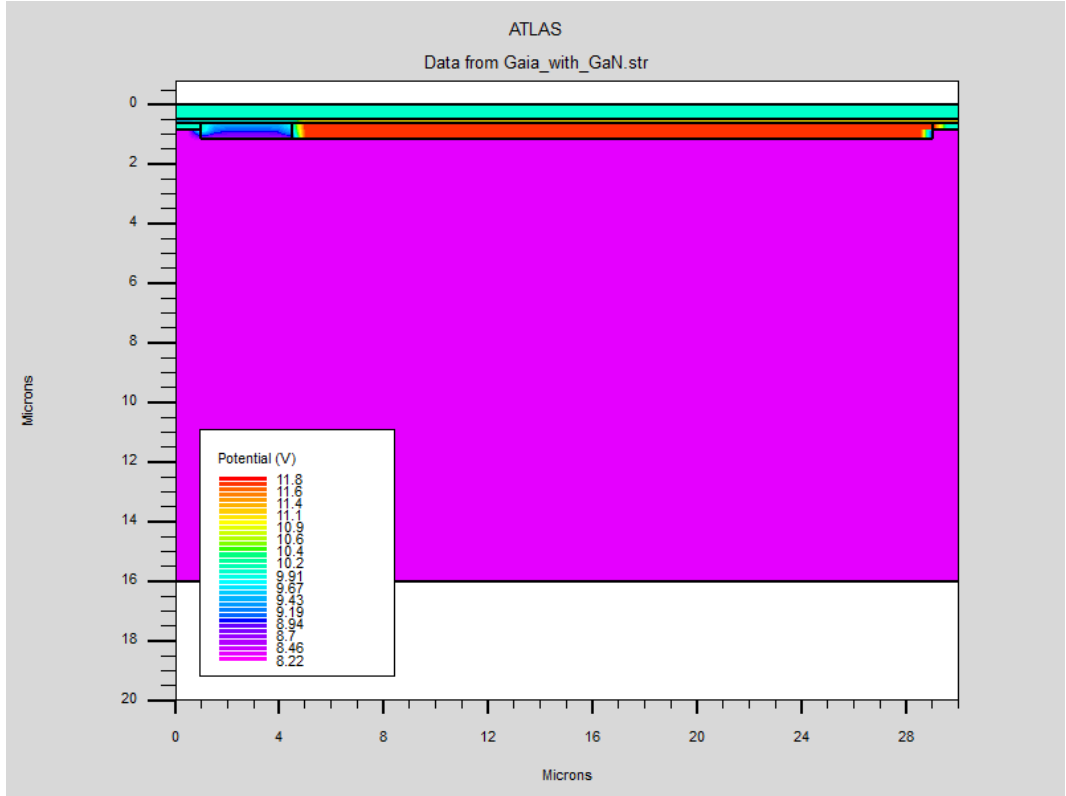


Fig. 6.2: The potential variation of the silicon Gaia AF CCD pixel model



**Fig. 6.3:** The potential variation of the GaN pixel model

It can be observed after comparing the above two figures that the maximum and minimum potentials for the silicon pixel model are 10.5 V and 9.61 V respectively. They are 11.8 V and 8.22 V for the GaN pixel model. This demonstrates that their electrical performances are in close comparison to each other.

To test the optical performance of both the models their IQE and EQE with and without suitable AR coatings have been calculated and compared in **Figs. 6.4 (a), (b), and (c)**. The thickness of the AR coating for the GaN model has been set to 86.3 nm and for the silicon model to about 85 nm. The coating materials and their thickness for both models have been derived from the studies presented in **Chapter 3**.

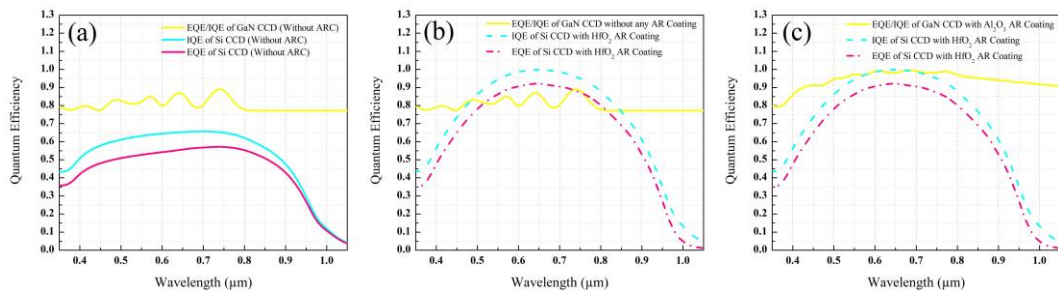


**Fig. 6.4:** Comparison of the IQE and EQE of the GaN model with the silicon pixel model when they are simulated (a) Without any AR coatings, (b) with only silicon model with an  $\text{HfO}_2$  coating, and (c) with GaN model with an  $\text{Al}_2\text{O}_3$  AR coating and silicon model with an  $\text{HfO}_2$  AR coating

The optical performance of the GaN model is as expected and much better than the silicon model in all three cases. When their optical performance is compared without any AR coatings the GaN pixel model provides an average increment of about 84.6 % in the EQE. An average increment of about 31.2 % is observed even when the GaN pixel structure without any AR coating is compared with the silicon model with an  $\text{HfO}_2$  AR coating. Finally, when both the models with an AR coating are compared, the average increment offered by the GaN pixel has been determined as 52.8 %.

---

For the GaN model, the differences in the EQE and IQE are very minute, of the order of  $10^{-3}$ . These negligible differences can be attributed to the fact that GaN has a better conductivity than silicon and after using the doping values mentioned above its conductivity increases even more [35]. For the silicon model, the doping values are not very high and hence the difference between its EQE and IQE is observed.

## 6.5 CONCLUSION

In astronomical parlance, the increment in the EQE and IQE values offered by the GaN pixel model is quite substantial. While the silicon-based broadband pixel model needs an AR coating to compete with an uncoated GaN pixel model, the GaN pixel still increases the QE by almost a third of the QE offered by the silicon model. Hence, the GaN CCDs can be used without an AR coating and still provide better results. This would also mean that long deliberations for an AR coating material for an astronomical CCD can be eliminated, saving time and simplifying the fabrication process. Even with such a substantial increment in the QE, GaN does not lag in its electrical performance. Hence, GaN can prove to be the future of astronomical CCDs and pave the path for a better exploration of the universe.

---

## CHAPTER 7

### CONCLUSION AND FUTURE SCOPE OF THIS WORK

We tested our Gaia AF CCD pixel model against the actual EQE values reported by Walker et al. (2008) using the Monte Carlo simulations of the SILVACO TCAD software. This has been done to ensure the accuracy of our simulations. It can be evidently seen in **Fig 4.4** that there are some differences between the experimental observations and our simulations. These deviations in the results might be attributed to the absence of SBC and ABD in our structure since these features are proprietary to e2v.

We studied the Gaia AF CCDs and tested them with various AR coatings to enhance their QE values. Our simulations establish that AR coatings are an important factor in improving the IQE and EQE of astronomical CCDs. They also elucidate that Ta<sub>2</sub>O<sub>5</sub> and ZrO<sub>2</sub> are better materials for astronomical CCDs than HfO<sub>2</sub>, mainly in the spectrum region from 0.330  $\mu\text{m}$  to 0.575  $\mu\text{m}$ . ZnS and Al<sub>2</sub>O<sub>3</sub>, although appear to be promising materials yet do not prove to be very efficient in enhancing the Gaia AF CCDs QE values.

Furthermore, due to the low absorption coefficient of silicon and large reflection losses in almost the whole operation of the Gaia AF CCDs GaN has been analysed electrically and optically to be considered as an alternative to silicon for

---

---

broadband astronomical CCDs. The GaN CCDs can prove to be substantially better than the silicon CCDs due to their superior optical and electrical performance.

This work has important implications for the development of astronomical CCDs, which will help them to obtain the best possible data from satellites and telescopes. Multi-layer AR coatings and the use of GaN as a material for the CCD substrate can be deliberated for this purpose in the future which can enhance our knowledge of the Milky Way and the universe even more. In this work, we focused on the optical losses of astronomical CCDs. For future studies, other losses of the CCDs such as dark current, trap formation, etc., can also be interpreted in depth which will help astronomers work in the direction of irradiating these losses and making CCDs more efficient and increasing their usefulness.

---

## REFERENCES

- [1] N. Alfaraj, "A review of charge-coupled device image sensors," *University of Toronto: Toronto, ON, Canada*, 2017.
- [2] M. Lesser, "Charge coupled device (CCD) image sensors," in *High Performance Silicon Imaging*: Elsevier, 2014, pp. 78-97.
- [3] M. Lesser, "A summary of charge-coupled devices for astronomy," *Publications of the Astronomical Society of the Pacific*, vol. 127, no. 957, pp. 1097-1104, 2015.
- [4] H. Rongqing, "Chapter 4 - Photodetectors," in *Introduction to Fiber-Optic Communications*, H. Rongqing Ed.: Academic Press, 2020, pp. 125-154.
- [5] I. Lundstrm, "Hydrogen sensitive MOS-structures: part 1: principles and applications," *Sensors and actuators*, vol. 1, pp. 403--426, 1981.
- [6] S. E. Holland, D. E. Groom, N. P. Palaio, R. J. Stover, and W. Mingzhi, "Fully depleted, back-illuminated charge-coupled devices fabricated on high-resistivity silicon," *IEEE Transactions on Electron Devices*, vol. 50, no. 1, pp. 225-238, 2003, doi: 10.1109/TED.2002.806476.
- [7] G. E. Smith, "Nobel Lecture: The invention and early history of the CCD," *Reviews of modern physics*, vol. 82, no. 3, p. 2307, 2010.
- [8] S. A. Taylor, "CCD and CMOS imaging array technologies: technology review," *UK: Xerox Research Centre Europe*, pp. 1-14, 1998.
- [9] R. H. Walden, R. H. Krambeck, R. J. Strain, J. McKenna, N. L. Schryer, and G. E. Smith, "B.S.T.J. brief: The buried channel charge coupled device," *The Bell System Technical Journal*, vol. 51, no. 7, pp. 1635-1640, 1972, doi: 10.1002/j.1538-7305.1972.tb02674.x.
- [10] B. E. Burke and S. A. Gajar, "Dynamic suppression of interface-state dark current in buried-channel CCDs," *IEEE Transactions on Electron Devices*, vol. 38, no. 2, pp. 285-290, 1991, doi: 10.1109/16.69907.



- 
- [11] M. Lesser, "Antireflection coatings for silicon charge-coupled devices," *Optical Engineering*, vol. 26, no. 9, pp. 911--921, 1987.
- [12] P. D. Omodeo, "Geocentrism," in *Encyclopedia of Renaissance Philosophy*: Springer International Publishing, 2016, pp. 1-6.
- [13] H. R. Devi, O. Y. Bisen, S. Nanda, R. Nandan, and K. K. Nanda, "Internal versus external quantum efficiency of luminescent materials, photovoltaic cells, photodetectors and photoelectrocatalysis.," *Current Science (00113891)*, vol. 127, no. 7, 2021.
- [14] M. Born and E. Wolf, *Principles of optics: electromagnetic theory of propagation, interference and diffraction of light*. Elsevier, 2013.
- [15] E. Hecht, "Optics 5th edn (England," ed: Pearson, 2017.
- [16] A. Walker *et al.*, "The Gaia challenge: Testing high performance CCDs in large quantities," 2008.
- [17] T. Prusti *et al.*, "The gaia mission," *Astronomy & astrophysics*, vol. 595, p. A1, 2016.
- [18] A. U. Manual, "Silvaco International," *Santa Clara, CA*, vol. 95054, p. 23, 2000.
- [19] I. Silvaco, "ATLAS user's manual device simulation software," *Santa Clara, CA*, 2010.
- [20] C. Crowley *et al.*, "Gaia data release 1-On-orbit performance of the Gaia CCDs at L2," *Astronomy & Astrophysics*, vol. 595, p. A6, 2016.
- [21] J. H. J. De Bruijne, "Science performance of Gaia, ESA's space-astrometry mission," *Astrophysics and Space Science*, vol. 341, no. 1, pp. 31--41, 2012.
- [22] G. Seabroke, A. Holland, and M. Cropper, "Modelling radiation damage to ESA's Gaia satellite CCDs," 2008.
- [23] G. M. Seabroke, A. D. Holland, D. Burt, and M. S. Robbins, "Modelling electron distributions within ESA's Gaia satellite CCD pixels to mitigate radiation damage," 2009.
- [24] G. Seabroke, A. Holland, D. Burt, and M. Robbins, "Silvaco ATLAS model of ESA's Gaia satellite e2v CCD91-72 pixels," 2010.
- [25] G. M. Seabroke, T. Prod'homme, G. Hopkinson, D. Burt, M. Robbins, and A. Holland, "Modelling Gaia CCD pixels with Silvaco 3D engineering
-

- 
- software," *European Astronomical Society Publications Series*, vol. 45, pp. 433--436, 2010.
- [26] W. Strehlow and E. L. Cook, "Compilation of energy band gaps in elemental and binary compound semiconductors and insulators," *Journal of Physical and Chemical Reference Data*, vol. 2, no. 1, pp. 163-200, 1973.
- [27] J. Krupka, J. Breeze, A. Centeno, N. Alford, T. Claussen, and L. Jensen, "Measurements of permittivity, dielectric loss tangent, and resistivity of float-zone silicon at microwave frequencies," *IEEE Transactions on microwave theory and techniques*, vol. 54, no. 11, pp. 3995-4001, 2006.
- [28] R. K. Chanana, "On the work function of metals and the electron affinity of crystal surfaces of semiconductors," *Journal of Electrical and Electronics Engineering*, vol. 17, no. 5, pp. 09-12, 2022.
- [29] D. V. Melnikov and J. R. Chelikowsky, "Electron affinities and ionization energies in silicon and Ge nanocrystals," *Physical Review B*, vol. 69, no. 11, p. 113305, 2004.
- [30] A. Aldalbahi *et al.*, "A new approach for fabrications of SiC based photodetectors," *Scientific Reports*, vol. 6, no. 1, p. 23457, 2016.
- [31] A. Gottwald, U. Kroth, E. Kalinina, and V. Zbrodskii, "Optical properties of a Cr/4H-SiC photodetector in the spectral range from ultraviolet to extreme ultraviolet," *Applied Optics*, vol. 57, no. 28, pp. 8431-8436, 2018.
- [32] M. L. Megherbi *et al.*, "An Efficient 4H-SiC photodiode for UV sensing applications," *Electronics*, vol. 10, no. 20, p. 2517, 2021.
- [33] F. Moscatelli, "Silicon carbide for UV, alpha, beta and X-ray detectors: Results and perspectives," *Nuclear Instruments and Methods in Physics Research Section A: Accelerators, Spectrometers, Detectors and Associated Equipment*, vol. 583, no. 1, pp. 157-161, 2007.
- [34] V. Sankin, P. Shkrebiy, and N. Savkina, "Silicon carbide ultraviolet photodetectors," in *International Semiconductor Device Research Symposium, 2003*, 2003: IEEE, pp. 130-131.
- [35] D. K. Saini, "Gallium nitride: Analysis of physical properties and performance in high-frequency power electronic circuits," Wright State University, 2015.
-

- 
- [36] N. Aggarwal and G. Gupta, "Enlightening gallium nitride-based UV photodetectors," *Journal of Materials Chemistry C*, vol. 8, no. 36, pp. 12348-12354, 2020.
- [37] O. Al-Zuhairi *et al.*, "Non-polar gallium nitride for photodetection applications: A systematic review," *Coatings*, vol. 12, no. 2, p. 275, 2022.
- [38] H. S. Alpert *et al.*, "Gallium nitride photodetector measurements of UV emission from a gaseous CH<sub>4</sub>/O<sub>2</sub> hybrid rocket igniter plume," in *2019 IEEE Aerospace Conference*, 2019: IEEE, pp. 1-8.
- [39] K. N. Chopra, "A Technical Note on Gallium Nitride Technology and short Qualitative Review of its Novel Applications," *Lat. Am. J. Phys. Educ. Vol*, vol. 8, no. 3, p. 541, 2014.
- [40] Z. Fan, "An analysis of GaN-based ultraviolet photodetector," in *IOP Conference Series: Materials Science and Engineering*, 2020, vol. 738, no. 1: IOP Publishing, p. 012006.
- [41] H. D. Jabbar, M. A. Fakhri, and M. J. AbdulRazzaq, "Gallium nitride-based photodiode: a review," *Materials Today: Proceedings*, vol. 42, pp. 2829-2834, 2021.

---

## DECLARATION

I hereby declare that the work which is presented in the Dissertation-II Project entitled “**Quantum Efficiency of Astronomical Charge-coupled Devices for Deeper Exploration of our Cosmos**” in the partial fulfilment of the requirement for the award of the Degree of **Masters in Science** and submitted to the Department of **Applied Physics**, Delhi Technological University, Delhi is an authentic record of my own, carried out during a period from August 2022 to May 2023, under the co-supervision of **Prof. (Dr.) Nitin K. Puri and Dr. George M. Seabroke**.

The matter presented in this thesis has not been submitted by me for the award of any other degree of this or any other Institute/ University. The work has been accepted and communicated in SCI/SCI Expanded indexed journals with the following details:

**Title of Paper 1: Diving deep into the Milky Way using Anti-Reflection Coatings for Astronomical CCDs**

**Author names (in sequence as per research paper):** Anmol Aggarwal, Ashi Mittal, George M. Seabroke, Nitin K. Puri

**Name of Journal:** Journal of Astrophysics and Astronomy

**Status of Paper (Accepted/Published/Communicated):** Accepted

**Date of paper communication:** 28<sup>th</sup> December 2022

**Date of paper acceptance:** 7<sup>th</sup> May 2023

**Title of Paper 2: Gallium Nitride: The future cornerstone of broad range astronomical CCDs**

**Author names (in sequence as per research paper):** Anmol Aggarwal, George M. Seabroke, Nitin K. Puri

**Name of Journal:** Experimental Astronomy

**Status of Paper (Accepted/Published/Communicated):** Communicated  
(Awaiting first report)

**Date of paper communication:** 27<sup>th</sup> July 2023



ANMOL AGGARWAL  
2K21/MSCPHY/55

---

## SUPERVISOR CERTIFICATE

To the best of our knowledge, the above work has not been submitted in part or full for any Degree or Diploma to this University or elsewhere. We further certify that the publication and indexing information given by the students is correct.

Place: Delhi



(Prof. Nitin K. Puri)

Date: 30 May 2023

Place: Newbury, United Kingdom



(Dr. George M. Seabroke)

Date: 30 May 2023

**NOTE: PLEASE ENCLOSE THE RESEARCH PAPER  
ACCEPTANCE/ PUBLICATION/COMMUNICATION  
PROOF ALONG WITH SCI INDEXING PROOF**

---

## **LIST OF PUBLICATIONS**

**Title of Paper 1: Diving deep into the Milky Way using Anti-Reflection Coatings for Astronomical CCDs**

**Author names (in sequence as per research paper):** Anmol Aggarwal, Ashi Mittal, George M. Seabroke, Nitin K. Puri

**Name of Journal:** Journal of Astrophysics and Astronomy

**Status of Paper (Accepted/Published/Communicated):** Accepted

**Date of paper communication:** 28<sup>th</sup> December 2022

**Date of paper acceptance:** 7<sup>th</sup> May 2023

**Title of Paper 2: Gallium Nitride: The future cornerstone of broad range astronomical CCDs**

**Author names (in sequence as per research paper):** Anmol Aggarwal, George M. Seabroke, Nitin K. Puri

**Name of Journal:** Experimental Astronomy

**Status of Paper (Accepted/Published/Communicated):** Communicated  
(Awaiting first report)

**Date of paper communication:** 27<sup>th</sup> July 2023

---

## ACCEPTANCE PROOF

### **Paper 1: Diving deep into the Milky Way using Anti-Reflection Coatings for Astronomical CCDs**

5/27/23, 11:03 PM Gmail - Fwd: JOAA: Your manuscript entitled Diving deep into the milky way using Anti-Reflection Coatings for Astronomical ...



Ashi Mittal <ashimittal2000@gmail.com>

---

#### **Fwd: JOAA: Your manuscript entitled Diving deep into the milky way using Anti-Reflection Coatings for Astronomical CCDs - [EMID:e43e6a967c22a3ff]**

1 message

---

**Dr. Nitin Puri** <nitinkumarpuri@dtu.ac.in>  
To: Ashi Mittal <ashimittal2000@gmail.com>, Anmol Aggarwal <stjadelhi@gmail.com>

15 May 2023 at 12:19

----- Forwarded message -----

From: **Annapurni Subramaniam** <em@editorialmanager.com>  
Date: Monday, May 8, 2023  
Subject: JOAA: Your manuscript entitled Diving deep into the milky way using Anti-Reflection Coatings for Astronomical CCDs - [EMID:e43e6a967c22a3ff]  
To: "Nitin K. Puri" <nitinkumarpuri@dtu.ac.in>

Ref.:  
Ms. No. JOAA-D-22-00278R1  
Diving deep into the milky way using Anti-Reflection Coatings for Astronomical CCDs  
Journal of Astrophysics and Astronomy

Dear Prof. Puri,

I am glad to inform you that your paper mentioned above has been accepted for publication in The Journal of Astrophysics and Astronomy.

The details are as follows:

Accepted 07 May 2023. Revised 09 Apr 2023. In original form 28 Dec 2022.

Regards,  
Chief Editor

Comments for the Author:

Reviewer #1: The changes previously suggested were carefully addressed and I do recommend the paper for publication.

---

In compliance with data protection regulations, you may request that we remove your personal registration details at any time. (Use the following URL: <https://www.editorialmanager.com/joaa/login.asp?a=r>). Please contact the publication office if you have any questions.

--  
**Dr. Nitin K. Puri**  
Professor, Department of Applied Physics,  
**Associate Dean (Outreach and Extension Activities)**  
Delhi Technological University (DTU)  
(Formerly Delhi College of Engineering, DCE)  
Govt. of NCT of Delhi  
Shahbad Daultapur, Main Bawana Road, Delhi-110042, India  
**Email:** [nitinkumarpuri@dtu.ac.in](mailto:nitinkumarpuri@dtu.ac.in)  
[www.dtu.ac.in](http://www.dtu.ac.in)

<https://mail.google.com/mail/u/0/?ik=a6dede7621&view=pt&search=all&permthid=thread-f:1765941802071750957&simpl=msg-f:1765941802071...> 1/1

# JOURNAL INDEXING PROOF

## Journal 1

Journal of Astrophysics and Astronomy  
Co-published by Indian Academy of Sciences and Astronomical Society of India

Editorial board | Aims & scope

Published by the Indian Academy of Sciences

**Editor-in-Chief**  
Annapurni Subramaniam

**Publishing model**  
Subscription

|                                      |  |                                   |
|--------------------------------------|--|-----------------------------------|
| <b>1.610 (2021)</b><br>Impact factor | <b>30 days</b><br>Submission to first decision<br>(Median) | <b>25,255 (2021)</b><br>Downloads |
|--------------------------------------|--|-----------------------------------|

**1.766 (2021)**  
Five year impact factor

You have access to our articles

**For authors**

[Submission guidelines](#)  
[Language editing services](#)  
[Ethics & disclosures](#)  
[Contact the journal](#)

Submit manuscript

**Electronic ISSN**  
0973-7758

**Co-Publisher information**  
Co-publication with Indian Academy of Sciences, Bangalore, India  
Visit Co-Publisher Site: [Astronomical Society of India](#) [Indian Academy of Sciences](#)

**Abstracted and indexed in**

|  |  |   |
|--|--|---|
| Astrophysics Data System (ADS)                         | EBSCO Discovery Service                      | Portico   |
| BFI List   | EBSCO Engineering Source                     | ProQuest Advanced Technologies & Aerospace Database |
| Baidu  | EBSCO STM Source                             | ProQuest-ExLibris Primo                             |
| CLOCKSS  | EBSCO Science & Technology Collection        | ProQuest-ExLibris Summon                            |
| CNKI   | Google Scholar                               | SCImago   |
| CNPIEC   | INIS Atomindex                               | SCOPUS  |
| Chemical Abstracts Service (CAS)                       | INSPEC                                       | Science Citation Index                              |
| Current Contents/Physical, Chemical and Earth Sciences | INSPIRE                                      | Science Citation Index Expanded (SCIE)              |
| Dimensions   | Japanese Science and Technology Agency (JST) | TD Net Discovery Service                            |
| EBSCO Academic Search                                  | Journal Citation Reports/Science Edition     | UGC-CARE List (India)                               |
| EBSCO Britannica Online Collection                     | Naver  | Wanfang   |
|  | OCLC WorldCat Discovery Service              |   |

**JOURNAL OF ASTROPHYSICS AND ASTRONOMY** [Share This Journal](#)

ISSN / eISSN 0250-6335 / 0973-7758  
Publisher INDIAN ACAD SCIENCES, C V RAMAN AVENUE, SADASHIVANAGAR, P B #8005, BANGALORE, INDIA, 560 080

**General Information**

|                          |                            |                           |         |
|--------------------------|----------------------------|---------------------------|---------|
| <b>Publisher Website</b> | <a href="#">Visit Site</a> | <b>1st Year Published</b> | 1980    |
| <b>Frequency</b>         | Continuous publication     | <b>Issues Per Year</b>    | 1       |
| <b>Country / Region</b>  | INDIA                      | <b>Primary Language</b>   | English |

**Web of Science Coverage**

| Collection      | Index                                  | Category                 |
|-----------------|--|--------------------------|
| Core Collection | Science Citation Index Expanded (SCIE) | Astronomy & Astrophysics |

Similar Journals [Find Similar Journals](#)



# Journal 2

https://www.springer.com/journal/10686

[Editorial board](#) [Aims & scope](#) [Journal updates](#)

*Experimental Astronomy* is a medium for the publication of papers on astrophysical instrumentation and methods throughout all five channels of information: Electromagnetic Radiation Astronomy, Solar System Observation and Exploration, Cosmic-Ray Detection, Neutrino Astronomy, and Gravitational-Wave Astronomy. — [show all](#)

**Editor-in-Chief**  
Peter von Ballmoos

**Publishing model**  
Hybrid (Transformative Journal). [How to publish with us, including Open Access](#)

|  |  |                                    |
|--|--|------------------------------------|
| <b>3.0 (2022)</b><br>Impact factor           | <b>20 days</b><br>Submission to first decision<br>(Median) | <b>164,437 (2022)</b><br>Downloads |
| <b>2.7 (2022)</b><br>Five year impact factor |  |                                    |

**You have access to our articles**

**For authors**

[Submission guidelines](#)  
[Language editing services](#)  
[Ethics & disclosures](#)  
[Open Access fees and funding](#)  
[Contact the journal](#)

Submit manuscript

**Working on a manuscript?**  
Avoid the most common mistakes and prepare your manuscript for journal editors.  
[Learn more](#) →

https://www.springer.com/journal/10686

**About this journal**

**Electronic ISSN** 1572-9508    **Print ISSN** 0922-6435

**Abstracted and indexed in**

|  |  |   |
|--|--|---|
| ANVUR  | EBSCO Discovery Service                      | Portico   |
| Astrophysics Data System (ADS)                         | EBSCO STM Source                             | ProQuest Advanced Technologies & Aerospace Database |
| BFI List   | Google Scholar                               | ProQuest-ExLibris Primo                             |
| Baidu  | INIS Atomindex                               | ProQuest-ExLibris Summon                            |
| CLOCKSS  | INSPEC                                       | SCImago   |
| CNKI   | INSPIRE                                      | SCOPUS  |
| CNPIEC   | Japanese Science and Technology Agency (JST) | Science Citation Index Expanded (SCIE)              |
| Current Contents/Physical, Chemical and Earth Sciences | Journal Citation Reports/Science Edition     | TD Net Discovery Service                            |
| Dimensions   | Naver  | UGC-CARE List (India)                               |
| EBSCO Academic Search                                  | OCLC WorldCat Discovery Service              | Wanfang   |

**Copyright information**  
[Rights and permissions](#)  
[Springer policies](#)

https://ml.darivate.com/journal-profile

Welcome, Anmol Aggarwal  
[Settings](#) [Log Out](#)

**Master Journal List**    [Search Journals](#)    [Match Manuscript](#)    [Downloads](#)    [Help Center](#)

Check out our new metric to help you evaluate journals!    [Dismiss](#)    [Learn More](#)

**EXPERIMENTAL ASTRONOMY**    [Share This Journal](#)

ISSN / eISSN 0922-6435 / 1572-9508  
Publisher SPRINGER, VAN GODEWIJKSTRAAT 30, DORDRECHT, NETHERLANDS, 3311 GZ

**General Information**

|                           |                            |                          |                            |
|---------------------------|----------------------------|--------------------------|----------------------------|
| <b>Journal Website</b>    | <a href="#">Visit Site</a> | <b>Publisher Website</b> | <a href="#">Visit Site</a> |
| <b>1st Year Published</b> | 1989                       | <b>Frequency</b>         | Bi-monthly                 |
| <b>Issues Per Year</b>    | 6                          | <b>Country / Region</b>  | NETHERLANDS                |
| <b>Primary Language</b>   | English                    |                          |                            |

[Return to Search Results](#)

# PLAGIARISM REPORT



Similarity Report ID: oid:2753536355986

PAPER NAME

**Thesis\_merged\_Anmol\_merged.pdf**

WORD COUNT

**9426 Words**

CHARACTER COUNT

**45801 Characters**

PAGE COUNT

**52 Pages**

FILE SIZE

**1.9MB**

SUBMISSION DATE

**May 28, 2023 6:43 PM GMT+5:30**

REPORT DATE

**May 28, 2023 6:43 PM GMT+5:30**

## 7% Overall Similarity

The combined total of all matches, including overlapping sources, for each database

- 4% Internet database
- 4% Publications database
- Crossref database
- Crossref Posted Content database
- 4% Submitted Works database

## Excluded from Similarity Report

- Bibliographic material
- Quoted material
- Cited material
- Small Matches (Less than 8 words)

Summary

**Prof. (Dr.) Nitin K. Puri**

**Supervisor**

**Anmol Aggarwal**

**2K21/MSCPHY/55**

**Dr. George M. Seabroke**

**Co-supervisor**

**Ashi Mittal**

**2K21/MSCPHY/07**



1

### 3 Diving deep into the milky way using anti-reflection coatings for astronomical 4 CCDs

5 ANMOL AGGARWAL<sup>1</sup>, ASHI MITTAL<sup>1</sup>, GEORGE M. SEABROKE<sup>2</sup> and  
6 NITIN K. PURI<sup>1,\*</sup>

7 <sup>1</sup>Advanced Sensor Laboratory and Nanomaterials Research Laboratory, Department of Applied Physics,  
8 Delhi Technological University, Delhi 110042, India.

9 <sup>2</sup>Mullard Space Science Laboratory, Department of Space and Climate Physics, Faculty of Maths and  
10 Physical Sciences, University College, London RH5 6NT, UK.

11 \*Corresponding author. E-mail: nitinkumarpuri@dtu.ac.in; nitinpuri2002@yahoo.co.in

12

13

MS received 28 December 2022; accepted 8 May 2023

14 **Abstract.** We report two anti-reflection (AR) coatings that give better quantum efficiency (9QE) than the  
15 existing AR coating on the Gaia astrometric field (AF) charged coupled devices (CCDs). Light being the core  
16 of optical astronomy, which is extremely important for such missions, therefore, the QE of the devices that  
17 are used to capture it should be substantially high. To reduce the losses due to the reflection of light from the  
18 surface of the CCDs, AR coatings can be applied. Currently, the main component of the Gaia satellite, the  
19 AF CCDs use hafnium dioxide (HfO<sub>2</sub>) AR coating. In this paper, the ATLAS module of the SILVACO  
20 software has been employed for simulating and studying the AF CCD pixel structure and several AR  
21 coatings. Our findings suggest that zirconium dioxide (ZrO<sub>2</sub>) and tantalum pentoxide (Ta<sub>2</sub>O<sub>5</sub>) will prove to  
22 be better AR coatings for broadband astronomical CCDs in the future and will open new avenues to  
23 understand the evolution of the milky way.

24

25

26

**Keywords.** gaia—sILVACO TCAD—astronomical instrumentation—charged coupled devices—anti-  
reflection coatings.

#### 27 1. Introduction

28 To enrich astronomy with more precise measure-  
29 ments, the European Space Agency (ESA) launched  
30 Gaia Satellite in the L2 orbit in December 2013. Its  
31 two telescopes keep an eye on millions of stars,  
32 galaxies and solar system objects to produce high-  
33 precision astrometric and spectroscopic measurements  
34 (Prusti *et al.* 2016). The continuous scan gives data  
35 sets that are repeatedly reduced to calculate the par-  
36 allax, position and proper motion of the celestial  
37 objects that are observed by the satellite (Crowley  
38 *et al.* 2016). The focal plane of the Gaia satellite  
39 contains 106 custom-built charged coupled devices  
40 (CCDs). These CCDs were designed and manufac-  
41 tured by e2v technologies, UK (Walker *et al.* 2008).

42 Gaia CCDs were fabricated by e2v in three different  
43 variants: Astrometric field (AF), red photometer (RP)  
44 and blue photometer (BP); each of these are optimized

45 for different wavelength ranges (De Bruijne 2012).  
46 The AF CCDs are built using silicon (Si) as a substrate  
47 with an anti-reflection (AR) coating, which has a  
48 maximum photon absorption for a light of 650 nm;  
49 this CCD has an extensive wavelength detection range  
50 of 330–1050 nm (Seabroke *et al.* 2008). There are 78  
51 AF CCDs on the Gaia focal plane, which are 16  $\mu$ m  
52 thick (Crowley *et al.* 2016). The BP and RP are  
53 enhanced CCDs that have exceptional sensitivity  
54 towards the blue (330–680 nm) and red (640–1050  
55 nm) regions of the light spectrum, respectively. Seven  
56 BP CCDs present on the Gaia focal plane, have the  
57 maximum photon absorption for the light of 360 nm  
58 because of its AR coating (Crowley *et al.* 2016).  
59 Correspondingly, seven RP CCDs have the maximum  
60 photon absorption for the light of 750 nm (Crowley  
61 *et al.* 2016). These CCDs have an image area of 4500  
62 lines  $\times$  1966 columns (here, lines and columns, refer  
63 to the rows and columns of the pixels of the CCD,

|                             |  |  |
|-----------------------------|--|--|
| Journal : Large 12036       | Dispatch : 7-6-2023                    | Pages : 9                                |
| Article No. : 9962          | <input type="checkbox"/> LE            | <input type="checkbox"/> TYPESET         |
| MS Code : JOAA-D-22-00278R1 | <input checked="" type="checkbox"/> CP | <input checked="" type="checkbox"/> DISK |

64 respectively) (De Bruijne 2012). A schematic diagram  
 65 of the arrangement of CCDs on the actual Gaia focal  
 66 plane is shown in figure 1. The detectors are operating  
 67 in the time delay and integration mode with a period  
 68 of 982.8  $\mu$ s, which synchronizes their line transfer rate  
 69 with the satellite rotation rate (Crowley *et al.* 2016; De  
 70 Bruijne 2012). In Gaia parlance, line transfer means  
 71 electrons being transferred in a row of pixels (Crowley  
 72 *et al.* 2016).

73 As the name suggests, AR coatings are essentially  
 74 important in improving the internal quantum effi-  
 75 ciency (IQE) of the CCDs because they play a vital  
 76 role in enhancing their photon absorption by reducing  
 77 the losses due to the reflection of incident light. The  
 78 IQE is used as a measuring stick to determine the  
 79 performance of an AR coating, which is the ratio of  
 80 the number of photons that enter the CCD to the  
 81 number of photons incident on the device (Devi *et al.*  
 82 2012). The external quantum efficiency (EQE) is the  
 83 ratio of the number of photoelectrons generated to the  
 84 number of photons incident on the CCD (Devi *et al.*  
 85 2012). Since the Gaia CCDs generally do not get a lot  
 86 of time to capture the incoming light from distant  
 87 objects, their IQE should be substantially high. An AR  
 88 coating is a thin layer of high refractive index material  
 89 (Lesser 1987). It also acts as a line of defence for the  
 90 CCDs (Lesser 1994).

91 The Gaia AF CCDs have been analysed since they  
 92 cover the maximum area (78 out of 106 CCDs) of the  
 93 Gaia focal plane and capture the widest wavelength  
 94 range. Studies that amalgamate AR coatings and  
 95 astronomical CCDs have been conducted. IQE of the  
 96 device has been deliberated, which in fact is directly

proportional to the EQE of the device. Several AR  
 coatings for the Gaia AF CCDs have been scrutinized  
 to enhance this factor using the SILVACO software. 99

2. Simulations and calculations 100

SILVACO TCAD is used to simulate several elec-  
 tronic and optical devices. It uses numerical methods  
 for simulations so that the development and opti-  
 mization of such devices can be expedited. For sim-  
 ulating the effects of AR coatings on an optoelectronic  
 device, the LUMINOUS and the ATLAS modules of  
 this software can be used. 107

Since the Gaia AF CCDs are back-illuminated  
 devices, the AR coatings are applied on the backside.  
 Photons are also fired on this side in our simulations.  
 The operating voltage was set to 10 V as suggested by  
 Seabroke *et al.* (2009). In SILVACO simulations, the  
 ratio of available current density ( $J_{available}$ ) and source  
 current density ( $J_{source}$ ) gives the IQE of a device. The  
 number of photoelectrons generated in a device can be  
 determined using the electron current density ( $J_n$ ). 116

We simulated an AF CCD pixel in 2-dimensions  
 (2D) using SILVACO, our aim is to obtain IQE of the  
 device with various AR coatings at different wave-  
 lengths. We assessed several materials as AR coat-  
 ings, namely, hafnium dioxide ( $HfO_2$ ), aluminum  
 oxide ( $Al_2O_3$ ), zinc sulfide (ZnS), zirconium dioxide  
 ( $ZrO_2$ ) and tantalum pentoxide ( $Ta_2O_5$ ). Although an  
 AR coating of  $HfO_2$  is already present on the AF  
 CCDs (Short *et al.* 2005), which gives impressive  
 results. We suspected that there was a scope of 126

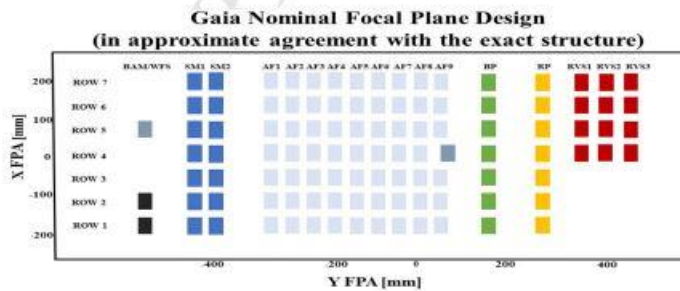


Figure 1. Gaia focal plane has 106 CCDs arranged in seven different rows. The red rectangles represent radial velocity spectrometers (RVS). The green and yellow rectangles depict blue and red photometers (BP and RP), respectively, while the grey and black rectangles show wavefront sensors (WFS) and basic angle monitors (BAM), respectively. The light blue rectangles depict the most abundant i.e., AF CCDs and the dark blue rectangles are called sky mappers (SM). The SM and the WFS are also AF CCDs. The RVS and BAM have a constructions similar to the RP.

|                            |  |  |
|----------------------------|--|--|
| Journal : Large 12036      | Dispatch : 7-6-2023                    | Pages : 9                                |
| Article No : 9962          | <input type="checkbox"/> LE            | <input type="checkbox"/> TYPESET         |
| MS Code : J03AA-02-00278R1 | <input checked="" type="checkbox"/> CP | <input checked="" type="checkbox"/> DISK |

127 improvement in IQE of the devices. Our simulations  
 128 proclaim that EQE of the Gaia AF CCDs with this AR  
 129 coating peaks at 650 nm with a value of 0.99. Simu-  
 130 lating these CCDs without any AR coating revealed  
 131 that there is a large increase of 37.2% in the IQE when  
 132 AR coatings are applied on such devices. Hence, AR  
 133 coatings can be regarded as a cornerstone of astro-  
 134 nomical CCDs.

135 A CCD is essentially a MOS-based device, which  
 136 acts as an image detector. In MOS, the letter M stands  
 137 for metal, the letter O stands for oxide and the letter S  
 138 stands for semiconductor (Lundström 1981). There-  
 139 fore, the structure of CCD consists of a layer of  
 140 metallic electrodes placed on a thin insulating layer  
 141 lined over a semiconductor substrate. Lundström  
 142 (1981) reports details of the MOS structure. CCDs are  
 143 of two types, front-illuminated and back-illuminated.  
 144 In the former, light is incident on the electrodes, while  
 145 the light is incident on the semiconductor substrate in  
 146 the latter (Lesser 2014, 2015). The back-illuminated  
 147 CCDs are constructed in actual practice because they  
 148 offer a larger surface area for photogeneration and  
 149 photon absorption than front-illuminated CCDs (Les-  
 150 ser 2015).

151 For simulating the Gaia AF CCD pixel in SIL-  
 152 VACO, several structural parameters were required,  
 153 which were derived from (Seabroke *et al.*  
 154 2008, 2009, 2010; Seabroke *et al.* 2010). The pixel  
 155 structure of the CCD has three different faces, which  
 156 is evident from figure 2. We simulated the structure in  
 157 the across scan (AC) direction in 2D with a pixel size  
 158 of  $16 \mu\text{m} \times 30 \mu\text{m}$ . The  $16 \mu\text{m}$  thickness of the pixel  
 159 is subdivided into multiple layers, the details of which  
 160 are summarized in Table 1.

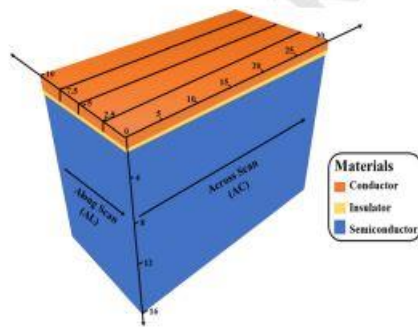


**Figure 2.** Structure of a single pixel of the Gaia AF CCD (all the measurements are in  $\mu\text{m}$ ).

161 The Gaia AF CCD entails a lot of interesting  
 162 structural intricacies, namely, buried channel (BC),  
 163 supplementary buried channel (SBC) and anti-  
 164 blooming drain (ABD) (Seabroke *et al.* 2008). A BC  
 165 is formed near a p–n junction by placing a thin layer  
 166 of negatively doped Si on a positively doped substrate.  
 167 This channel has no free charges and is used to hold  
 168 the photogenerated electrons before they are read out.  
 169 A photon incident on a CCD creates an electron–hole  
 170 pair; the electron thus generated, then moves to the  
 171 BC.

172 The SBC is a support feature to the BC but is no  
 173 less functional. When the number of photogenerated  
 174 electrons exceeds the capacity of the SBC, they spill  
 175 into the BC which holds them until they are read out  
 176 (Seabroke *et al.* 2010, 2013). The length of BC and  
 177 SBC runs from 4.5 to  $29 \mu\text{m}$  in the AC direction  
 178 (Seabroke *et al.* 2010). The ABD, which is present on  
 179 either side of the pixel in the AC direction is a  
 180 shielding feature. It prevents the electrons from  
 181 divulging into the adjacent pixel (Seabroke *et al.*  
 182 2010). Now, to simulate all these interesting features  
 183 in SILVACO, the whole AF CCD image pixel was  
 184 modeled with uniform doping as suggested by Sea-  
 185 broke *et al.* (2009).

186 The Gaia AF CCDs work at a temperature of 163 K  
 187 (Seabroke *et al.* 2008) to minimize the dark current,  
 188 which is attributed to the false positive signals pro-  
 189 duced in the CCD due to the thermal energy of elec-  
 190 trons (Lesser 2015). Therefore, to match our  
 191 theoretical simulations with the experimental results  
 192 reported by Walker *et al.* (2008), we conducted our  
 193 simulations at the same temperature.

194 To simulate the CCD pixel structure, the SILVACO  
 195 ATLAS package uses some constants for the simu-  
 196 lated materials that are handled internally. It uses the  
 197 Monte Carlo method to model the structure. Table 2  
 198 compares the experimental values of the constants  
 199 with the values used during our simulations.

200 Figure 3 exhibits the simulated structure of the Gaia  
 201 AF CCD pixel; the illustration was generated using  
 202 the TonyPlot tool of the SILVACO software.

### 2.1 AR coatings

204 We have elucidated the Gaia AF CCD pixel structure  
 205 used in our simulations, but to test their efficiency, the  
 206 IQE can be used. To begin with, we have focused on  
 207 single-layer AR coatings that have been applied on the  
 208 backside of the CCD (substrate side). The thickness of

**Table 1.** Thickness and doping densities of different layers in the AF CCD pixel structure (Seabroke *et al.* 2009).

| S. no. | Material                           | Type          | Thickness ( $\mu\text{m}$ ) | Doping density ( $\text{cm}^{-3}$ ) |
|--------|------------------------------------|---------------|-----------------------------|-------------------------------------|
| 1      | Polycrystalline Si                 | Conductor     | 0–0.5                       | 0                                   |
| 2      | Silicon dioxide ( $\text{SiO}_2$ ) | Insulator     | 0.5–0.63                    | 0                                   |
| 3      | N-type Si                          | Semiconductor | 0.63–1.17                   | $2.65 \times 10^{16}$               |
| 4      | P-type Si                          | Semiconductor | 1.17–16                     | $1.3 \times 10^{14}$                |

**Table 2.** List of theoretical and experimental constants.

| S. no. | Name of constant                             | Theoretical values used in SILVACO ATLAS | Experimental values  |
|--------|--|--|--|
| 1.     | Energy gap of Si ( $E_g$ )                   | 1.08 eV at 300 K<br>1.11 eV at 163 K     | 1.12 eV at 300 K (Strehlow & Cook 1973)                      |
| 2.     | Relative permittivity of Si ( $\epsilon_r$ ) | 11.8 at 300 K<br>11.8 at 163 K           | 11.66 at 300 K (Krupka <i>et al.</i> 2006)                   |
| 3.     | Electron affinity of Si ( $X$ )              | 4.17 eV at 300 K<br>4.16 eV at 163 K     | 4.05 eV at 300 K (Melnikov & Chelikowsky 2004; Chanana 2022) |
| 4.     | Temperature ( $T$ )                          | 163 K                                    | 163 K (Seabroke <i>et al.</i> 2008)                          |

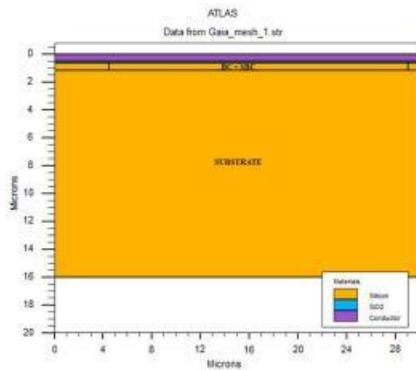


**Figure 3.** 2D Gaia AF CCD structure in the across scan (AC) direction as simulated in SILVACO ATLAS.

209 the AR coating is estimated using the quarter wave-length formula (Equation 1).

$$\text{AR coating thickness} = \frac{\lambda}{4n} \quad (1)$$

212 In Equation (1),  $\lambda$  is the wavelength at which the  
213 AR coating is centered, i.e., the wavelength at which  
214 the AR coating will allow for maximum photon  
215 absorption;  $n$  is the refractive index of the AR coating  
216 material at the wavelength  $\lambda$  (Lesser 1987). The

SOPRA database of the SILVACO ATLAS software 217  
was tremendously helpful in allowing us to include the  
218 refractive indices of the AR coatings. When the  
219 refractive index of AR coatings at a specified wave-  
220 length comes in approximate agreement with  $\sqrt{n}$ ,  
221 where  $n$  is the refractive index of the substrate material  
222 at that wavelength, then, we get excellent IQE  
223 values. To choose an AR coating, this factor was  
224 deliberated.

225  
226 On comparing the values of refractive indices of  
227 various AR coatings with the  $\sqrt{n}$ , at different  
228 wavelengths, we got some AR coatings whose  
229 refractive indices match the  $\sqrt{n}$  values and promise  
230 good results in IQE. In figure 4, we can see the  
231 comparison of  $\text{HfO}_2$  coating's refractive indices with  
232 the square root values of Si refractive indices. There  
233 is a very good matching which evidently explains  
234 why this AR coating is used in designing the Gaia  
235 AF CCDs.

236 On performing the same comparison with various  
237 AR coatings, we got some promising results from  
238 ZnS,  $\text{Al}_2\text{O}_3$ ,  $\text{ZrO}_2$  and  $\text{Ta}_2\text{O}_5$ , which can be seen in  
239 figure 5. Figure 5a shows how similar the values of  
240  $\sqrt{n}$  of Si and the refractive index of ZnS. Figure 5b  
241 shows that the refractive index of  $\text{Al}_2\text{O}_3$  is also close  
242 to the  $\sqrt{n}$  of Si values. Figure 5c and d show similar  
243 results for  $\text{ZrO}_2$  and  $\text{Ta}_2\text{O}_5$ .

244 While choosing the materials for AR coatings, their  
245 imaginary refractive index, which is a complex optical

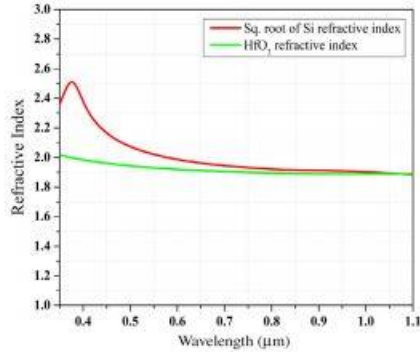


**Figure 4.** Comparison of the refractive index of HfO<sub>2</sub> with the square root of the refractive index of Si at different wavelengths.

constant, often referred to as the extinction coefficient 246  
has also been considered. Using this, we can calculate 247  
the absorption coefficient ( $\alpha$ ), which is the distance a 248  
photon can travel into the material before being 249  
absorbed. It is given by Equation (2): 250

$$\text{Absorption coefficient } (\alpha) = \frac{4\pi k}{\lambda}, \quad (2)$$

where  $\lambda$  is the wavelength of incident light. We 252  
calculated the values of  $\alpha$  for whole wavelength 253  
range of the Gaia astrometric field (AF) CCD using 254  
SILVACO ATLAS with different AR coatings, 255  
which are presented in figure 6(a-c). It can be 256  
concluded from these results that the AR coatings 257  
have no effect on the absorption coefficient of sil- 258  
icon (Si). 259

Another factor that has been deliberated while 260  
selecting the AR coating material is reflectivity ( $R_0$ ). 261

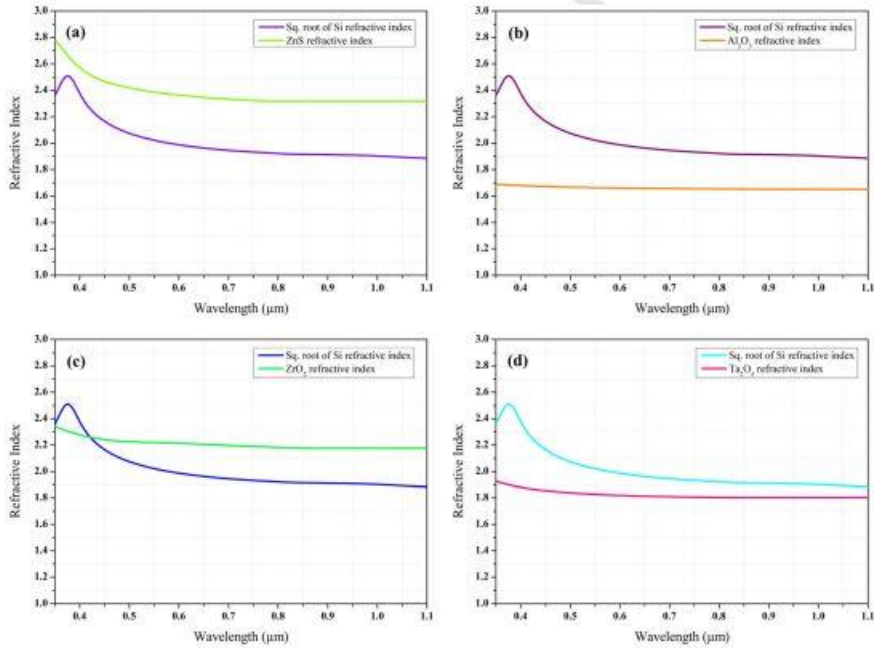


**Figure 5.** Comparison of the square root of the refractive index of Si with a ZnS, b Al<sub>2</sub>O<sub>3</sub>, c ZrO<sub>2</sub> and d Ta<sub>2</sub>O<sub>5</sub> at different wavelengths.

|                            |  |  |
|----------------------------|--|--|
| Journal : Large 12036      | Dispatch : 7-6-2023                    | Pages : 9                                |
| Article No. : 5962         | <input type="checkbox"/> LE            | <input type="checkbox"/> TYPESET         |
| MS_Code : J03AA-02-00758R1 | <input checked="" type="checkbox"/> CP | <input checked="" type="checkbox"/> DISK |

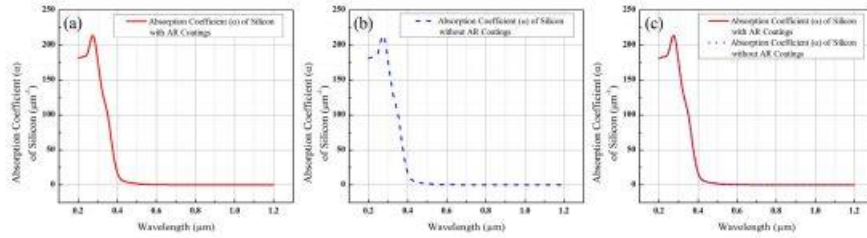


**Figure 6.** Absorption coefficient of Si: **a** with AR coatings, **b** without AR coatings and **c** with and without AR coatings.

Equation (3) is used to calculate the reflectivity of a surface using the real refractive indices:

$$R_0 = \left( \frac{n_1 - n_2}{n_1 + n_2} \right)^2 \quad (3)$$

where  $n_1$  and  $n_2$  are the real refractive indices (at a specific wavelength) of the medium from which the light is incident and the AR coating material, respectively. The reflectivity of the Si-air interface is largely affected by the optical properties of AR coating materials. The effect of AR coatings on the reflectivity of the Si-air interface is presented in figure 7, which has been calculated using the SILVACO ATLAS software.

For an AR coating to perform well, its respective refractive indices of the AR coating material also should be in approximate agreement with the square root of the respective refractive indices of the substrate material ( $\sqrt{n}$ ), as per Lesser (1987).  $Ta_2O_5$  satisfies this condition, is the best among all the

studied AR coating materials, and reduces the reflectivity substantially. Hence, it can be concluded that  $Ta_2O_5$  can be proven to be the best AR coating material for our case. Although  $Al_2O_3$  reduces the reflectivity to the least value compared to all the studied AR coatings, as presented in figure 7, its respective refractive indices are not very close to the square root of the respective refractive indices of Si (figure 5b), which might hinder its performance.

### 3. Results and discussion

While simulating the pixel structure with the  $HfO_2$  AR coating, Equation (1) deduces the thickness of the coating to 0.085  $\mu m$ . We identified the EQE for this setup to benchmark our simulations against the previously published EQE values by Walker *et al.* (2008). The simulation results are comparable to the experimental results, which can be visualized in figure 8(a). Any differences in the values of EQE might be because of the absence of ABD in our structure, as the parameters required for its simulations were not published in the current literature.

On calculating IQE for the Gaia AF CCD without applying any AR coating, it was discovered that they have a maximum IQE of 0.65 at the wavelength of 0.7  $\mu m$ . Comparing the IQE of the CCDs with and without the  $HfO_2$  coating, we clearly observed an average increment of about 37.2% in the whole wavelength range. Figure 8b conveys this increment graphically.

As per our study of AR coating materials, we choose four AR coatings to test our device. One of them is ZnS. Application of 0.069  $\mu m$  thick single-layer coating of ZnS, centered at 0.65  $\mu m$ , unfolds that it is not very suitable for our device. The IQE curve in figure 8c outlines that there is an average decrement of ~3.5% when studied parallel to the Gaia AF CCD with a  $HfO_2$  AR coating in the whole range.

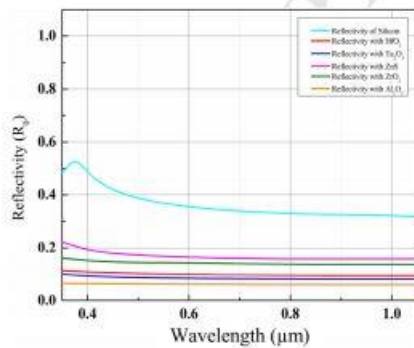


**Figure 7.** Reflectivity of the CCD surface without any AR coating and with different AR coatings.

|                              |  |  |
|------------------------------|--|--|
| Journal : Large 12036        | Dispatch : 7-6-2023                    | Pages : 9                                |
| Article No. : 9962           | <input type="checkbox"/> LE            | <input type="checkbox"/> TYPESET         |
| MS Code : IOAA-42-32-00720R1 | <input checked="" type="checkbox"/> CP | <input checked="" type="checkbox"/> DISK |



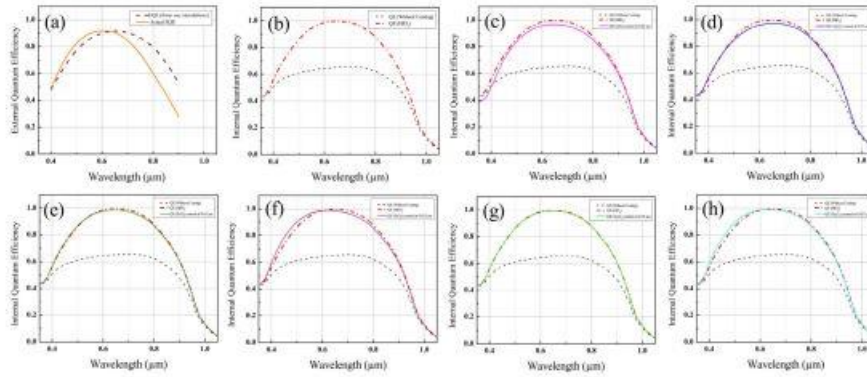


**Figure 8.** a EQE of the Gaia AF CCDs derived from our simulations and the actual EQE reported by Walker *et al.* (2008). The IQE versus wavelength graph for Gaia AF CCD, b without an AR coating and with a HfO<sub>2</sub> coating (centered at 0.65 μm), c ZnS coating (centered at 0.65 μm), d Al<sub>2</sub>O<sub>3</sub> coating (centered at 0.65 μm), e ZrO<sub>2</sub> coating (centered at 0.65 μm), f ZrO<sub>2</sub> coating (centered at 0.625 μm), g Ta<sub>2</sub>O<sub>5</sub> coating (centered at 0.65 μm) and h Ta<sub>2</sub>O<sub>5</sub> coating (centered at 0.625 μm).

316 Our next choice was Al<sub>2</sub>O<sub>3</sub>. Therefore, we applied a  
 317 single layer of it with a thickness of about 0.098 μm  
 318 (calculated as per Equation 1), centered at 0.65 μm.  
 319 The Gaia AF CCD with HfO<sub>2</sub> AR coating still  
 320 provides better results for most wavelengths as compared  
 321 to Al<sub>2</sub>O<sub>3</sub>. It is also observed that Al<sub>2</sub>O<sub>3</sub> coating  
 322 provides an average improvement in IQE of about 1.3%  
 323 in the 0.35–0.425 μm range and an average decrement  
 324 of about 1.9% in the rest of the wavelength range.  
 325 These results are compiled in the graph presented in  
 326 figure 8d.  
 327 The next alternative that we analysed was a single-  
 328 layer coating of ZrO<sub>2</sub> centered at 0.65 μm. The  
 329 thickness of the coating was set as per Equation (1)  
 330 close to 0.073 μm. After observing the graphical data  
 331 presented in figure 8e, we infer that there is an average  
 332 increment in the IQE of around 0.8% in the range of  
 333 0.4–0.525 μm when analogized with the IQE values  
 334 when HfO<sub>2</sub> coating was applied. For the rest of the  
 335 wavelengths, the AR coating of HfO<sub>2</sub> offers an average  
 336 increment of almost 1.1%, when compared to  
 337 ZrO<sub>2</sub>.  
 338 Inspired by the improvements shown by ZrO<sub>2</sub>, we  
 339 adjusted its thickness to an approximate value of  
 340 0.071 μm, which allows for a peak absorbance of the  
 341 light of wavelength of 0.625 μm. Our experimentation  
 342 on this, yields an average increment of nearly 4% for  
 343 the wavelength range of 0.375–0.575 μm when

344 compared with HfO<sub>2</sub>, with an average compromise of  
 345 around 2% in the wavelength range of 0.575–1.05 μm.  
 346 This data is visualized in figure 8f.  
 347 We concluded our studies with Ta<sub>2</sub>O<sub>5</sub>, which is a  
 348 promising AR coating. A single layer of Ta<sub>2</sub>O<sub>5</sub>, cen-  
 349 tered at 0.65 μm with a thickness of ~0.09 μm (cal-  
 350 culated using Equation 1), permits almost the same  
 351 performance as HfO<sub>2</sub>. It is evident from figure 8g that  
 352 the two curves virtually overlap each other in the  
 353 whole range. We did not obtain such promising results  
 354 for any other AR coating. Hence, to improve the IQE  
 355 in the low wavelength region, we deposited a 0.086  
 356 μm thick layer of Ta<sub>2</sub>O<sub>5</sub> to the center of the AR  
 357 coating at 0.625 μm. The IQE of the Gaia AF CCDs  
 358 with an AR coating of Ta<sub>2</sub>O<sub>5</sub> shows an average  
 359 increment of about 2.8% compared to the CCDs with  
 360 HfO<sub>2</sub> AR coating in the wavelength range of  
 361 0.375–0.6 μm. There is an average decrease of around  
 362 1.2% in IQE of the wavelengths ranging from 0.6 μm  
 363 to 1.05 μm, which is clearly evident in figure 8h.  
 364 A comparative study has been drawn to analyse,  
 365 which AR coating best suits the Gaia AF CCDs. It is  
 366 observed that a single layer coating of ZrO<sub>2</sub> and  
 367 Ta<sub>2</sub>O<sub>5</sub> gives similar or better results as compared to  
 368 HfO<sub>2</sub> for most wavelengths lying in Gaia's AF CCD  
 369 range (330–1050 nm) (Seabroke *et al.* 2008). Table 3  
 370 summarizes the comparison among the IQE of CCDs  
 371 for different AR coatings.

|                              |  |  |
|------------------------------|--|--|
| Journal : Large 12036        | Dispatch : 7-6-2023                    | Pages : 9                                |
| Article No : 9962            | <input type="checkbox"/> LE            | <input type="checkbox"/> TYPESET         |
| MS Code : JAAA-40-32-00278R1 | <input checked="" type="checkbox"/> CP | <input checked="" type="checkbox"/> DISK |

**Table 3.** Percentage increment and decrement in QE of the Gaia AF CCD with different AR coatings as compared to the HfO<sub>2</sub> AR coating.

| S. no. | AR coatings   | Wavelength range (μm) | Percentage increment/decrement in IQE                             | Average increment/decrement in IQE                            |
|--------|---|-----------------------|---|---|
| 1.     | HfO <sub>2</sub>                                      | 0.33–1.05             | Increment (2.6–53.3%) as compared to a CCD without any AR coating | Increment (37.2%) as compared to a CCD without any AR coating |
| 2.     | ZnS (centered at 0.65 μm)                             | 0.35–1.05             | Decrement (0.3–12.2%) as compared to HfO <sub>2</sub>             | Decrement (3.5%) as compared to HfO <sub>2</sub>              |
| 3.     | Al <sub>2</sub> O <sub>3</sub> (centered at 0.65 μm)  | 0.35–0.425            | Increment (0.1–2.3%) as compared to HfO <sub>2</sub>              | Increment (1.3%) as compared to HfO <sub>2</sub>              |
|        |   | 0.425–1.05            | Decrement (0.09–2.8%) as compared to HfO <sub>2</sub>             | Decrement (1.9%) as compared to HfO <sub>2</sub>              |
| 4.     | ZrO <sub>2</sub> (centered at 0.65 μm)                | 0.4–0.525             | Increment (0.04–1.35%) as compared to HfO <sub>2</sub>            | Increment (0.8%) as compared to HfO <sub>2</sub>              |
|        |   | 0.525–1.05            | Decrement (0.19–1.4%) as compared to HfO <sub>2</sub>             | Decrement (1.1%) as compared to HfO <sub>2</sub>              |
| 5.     | ZrO <sub>2</sub> (centered at 0.625 μm)               | 0.375–0.575           | Increment (0.63–6.85%) as compared to HfO <sub>2</sub>            | Increment (4%) as compared to HfO <sub>2</sub>                |
|        |   | 0.575–1.05            | Decrement (0.38–2.72%) as compared to HfO <sub>2</sub>            | Decrement (2%) as compared to HfO <sub>2</sub>                |
| 6.     | Ta <sub>2</sub> O <sub>5</sub> (centered at 0.65 μm)  | 0.35–0.9              | Decrement (0.64% and less) as compared to HfO <sub>2</sub>        | No prominent change as compared to HfO <sub>2</sub>           |
|        |   | 0.9–1.05              | Increment (0.04% and less) as compared to HfO <sub>2</sub>        | No prominent change as compared to HfO <sub>2</sub>           |
| 7.     | Ta <sub>2</sub> O <sub>5</sub> (centered at 0.625 μm) | 0.375–0.6             | Increment (0.17–5.15%) as compared to HfO <sub>2</sub>            | Increment (2.8%) as compared to HfO <sub>2</sub>              |
|        |   | 0.6–1.05              | Decrement (0.19–1.57%) as compared to HfO <sub>2</sub>            | Decrement (1.2%) as compared to HfO <sub>2</sub>              |

372 **4. Conclusions**

373 We tested our Gaia AF CCD pixel model against the  
 374 actual EQE values reported by Walker *et al.* (2008),  
 375 which indicated the accuracy of our simulations. We  
 376 presented our studies of the Gaia AF CCDs with  
 377 various AR coatings to enhance the QE values. Any  
 378 deviations in the results might be attributed to the  
 379 absence of SBC and ABD in our structure since these  
 380 features are proprietary to e2v. The performance of an  
 381 AR coating can also be determined using a simple Si  
 382 wafer. But, to validate our results for astronomical  
 383 CCDs, we used an electrical model in SILVACO  
 384 ATLAS. This allows our results to be more accept-  
 385 able to the astronomical community.

386 Our simulations establish that AR coatings are an  
 387 important factor in improving the IQE and EQE of  
 388 astronomical CCDs. They also elucidate that Ta<sub>2</sub>O<sub>5</sub>  
 389 and ZrO<sub>2</sub> are better materials for astronomical CCDs  
 390 than HfO<sub>2</sub>, mainly in the spectrum region from 0.330  
 391 μm to 0.575 μm. Hence, this work has important  
 392 implications for the development of astronomical

393 CCDs, which will help them to obtain the best possible  
 394 data from satellites and telescopes. Multi-layer  
 395 AR coatings can be deliberated for this purpose in the  
 396 future, which might enhance our knowledge of the  
 397 milky way even more.

398 **Acknowledgments**

399 We are grateful to Prof. Ashutosh Bharadwaj, Univer-  
 400 sity of Delhi, for his help and motivation throughout  
 401 this research. We are also thankful to Dr Harsupreet  
 402 Kaur for providing us with the license for TCAD  
 403 SILVACO ATLAS 2021 software. We gratefully  
 404 acknowledge Ms. Ritika Khatri, Delhi Technological  
 405 University, for her continuous support and guidance  
 406 during this research.

407 **References**

408 Chanana R. K. 2022, Journal of Electrical and Electronics  
 409 Engineering 17, 09

|                             |  |  |
|-----------------------------|--|--|
| Journal : Large 12036       | Dispatch : 7-6-2023                    | Pages : 9                                |
| Article No. : 9962          | <input type="checkbox"/> LE            | <input type="checkbox"/> TYPESET         |
| MS Code : JAAA-D-22-00275R1 | <input checked="" type="checkbox"/> CP | <input checked="" type="checkbox"/> DISK |

410 Crowley C., Kohley R., Hambly N. C. *et al.* 2016, *A&A* 595, A6  
411 De Bruijne J. 2012, *Ap&SS* 341, 31  
412 Devi H. R., Bisen O. Y., Nanda S., Nandan R., Nanda K. K.  
413 2021, *Current Science* 00113891, 127  
414 Krupka J., Breeze J., Centeno A. *et al.* 2006, *IEEE Transac-*  
415 *tions on Microwave Theory and Techniques* 54, 3995  
416 Lesser M. 1987, *Optical Engineering* 26, 911  
417 Lesser M. 2014, in *High Performance Silicon Imaging*  
418 (Elsevier), p. 78  
419 Lesser M. 2015, *PASP* 127, 1097  
420 Lesser M. P. 1994, in *Instrumentation in Astronomy VIII*,  
421 Vol. 2198, SPIE, p. 782  
422 Lundström I. 1981, *Sensors and Actuators* 1, 403  
423 Melnikov D. V., Chelikowsky J. R. 2004, *Physical Review*  
424 B 69, 113305  
425 Prusti T., De Bruijne J., Brown A. G. *et al.* 2016, *A&A* 595, A1  
426 Seabroke G., Holland A., Burt D., Robbins M. 2009, in  
427 *Astronomical and Space Optical Systems*, Vol. 7439, SPIE,  
428 p. 35  
Seabroke G., Holland A., Burt D., Robbins M. 2010, in  
429 *High Energy, Optical, and Infrared Detectors for Astron-*  
430 *omy IV*, Vol. 7742, SPIE, p. 339  
431 Seabroke G., Holland A., Cropper M. 2008, in *High*  
432 *Energy, Optical, and Infrared Detectors for Astronomy*  
433 *III*, Vol. 7021, SPIE, p. 515  
434 Seabroke G., Prod'homme T., Hopkinson G., *et al.* 2010,  
435 *European Astronomical Society Publications Series*, 45,  
436 433  
437 Seabroke G., Prod'homme T., Murray N., *et al.* 2013,  
438 *MNRAS*, 430, 3155  
439 Short A., Hopkinson G., Laborie A., *et al.* 2005, in *Focal*  
440 *Plane Arrays for Space Telescopes II*, Vol. 5902, SPIE,  
441 p. 31  
442 Strehlow W., Cook E. L. 1973, *Journal of Physical and*  
443 *Chemical Reference Data* 2, 163  
444 Walker A., Eaton T., Steward R., *et al.* 2008, in *Sensors,*  
445 *Systems, and Next Generation Satellites XII*, Vol. 7106,  
446 SPIE, p. 390  
447  
448

UNCORRECTED PROOF

|                             |  |  |
|-----------------------------|--|--|
| Journal : Large 12036       | Dispatch : 7-6-2023                    | Pages : 9                                |
| Article No. : 9962          | <input type="checkbox"/> LE            | <input type="checkbox"/> TYPESET         |
| MS Code : JOAA-D-23-00278R1 | <input checked="" type="checkbox"/> CP | <input checked="" type="checkbox"/> DISK |

---

## COMMUNICATED RESEARCH ARTICLE

### Gallium Nitride: The future cornerstone of broad range astronomical CCDs

Anmol Aggarwal<sup>a</sup> (ORCID ID: 0000-0003-3666-8873), George M. Seabrook<sup>b</sup> (ORCID ID: 0000-0003-4072-9536), Nitin K. Puri<sup>a\*</sup> (ORCID ID: 0000-0003-2563-3747)

<sup>a</sup> Advanced Sensor Laboratory & Nanomaterials Research Laboratory, Department of Applied Physics, Delhi Technological University, Delhi, 110042, India.

<sup>b</sup> Mullard Space Science Laboratory, Department of Space & Climate Physics, Faculty of Maths & Physical Sciences, University College, London, RH5 6NT, United Kingdom.

\*Corresponding Author, email id: nitinkumarpuri@dtu.ac.in, nitinpuri2002@yahoo.co.in

#### Abstract

All astronomical missions use charge-coupled devices (CCDs) as vital organs. Usually, silicon (Si) is selected to build them, which does not perform well without enhancements such as anti-reflection (AR) coatings. Such devices exhibit poor performance in the high (> 800 nm) and low (< 500 nm) wavelength ranges even with AR coatings. We present studies that signify gallium nitride (GaN) as a replacement for silicon (Si) in astronomical CCDs that operate in a wide wavelength range. For this purpose, SILVACO TCAD software has been employed, which has been used for simulating and comparing a GaN CCD pixel with a Gaia astrometric field (AF) CCD pixel. Our observations demonstrate that the optical performance of the GaN-based CCD pixel is remarkably better than the Si-based AF CCD pixel. These findings can prove to be the bedrock of future astronomical exploration and wide-range astronomical CCDs, as they allow for an exceptionally high quantum efficiency (QE) even without any reinforcements.

**Keywords:** Astronomical instrumentation, Gaia, Charge-coupled devices, Quantum Efficiency, Optics

#### Statements and Declarations

**Competing Interests:** The authors have no relevant financial or non-financial interests to disclose.

**Funding:** The authors declare that no funds, grants, or other support were received during the preparation of this manuscript.

1